Geophysical Journal International

*Geophys. J. Int.* (2023) **234,** 1531–1549 https://doi.org/10.1093/gji/ggad129
Advance Access publication 2023 March 22
GJI Geodynamics and Tectonics

# The Holy Cross Mountains (Poland) terranes palaeoposition and depositional environment in Silurian—new insights from rock magnetic studies

D.K. Niezabitowska [1,2] and R. Szaniawski[1]

[1] *Department of Magnetism, Księcia Janusza St.* 64, 01-452 *Warsaw, Poland. E-mail:* *dominika.niezabitowska@geo.uu.se*
[2] *Department of Earth Sciences, Uppsala University,* 752 36 *Uppsala, Sweden*

Accepted 2023 March 17. Received 2023 March 13; in original form 2023 January 27

## SUMMARY

The Holy Cross Mountains (HCM) in Poland, is an isolated natural outcrop of Palaeozoic rocks located within the Trans-European Suture Zone, a tectonic collage of continental terranes adjacent to the Tornquist margin of the Baltica. This uniqueness made the HCM a target for palaeogeographic research. Based on the facies differences, the HCM had been divided into two major units, the southern (the Kielce Unit) and northern (the Łysogóry Unit) part (SHCM and NHCM, respectively). Their position in relation to each other and the Baltica continent during Silurian times is still a matter of discussion, whether both parts of the HCM were separated terranes located along the Baltica margin or they shared in common palaeogeographic history. Here, we present the results of comprehensive rock magnetic measurements applied as a tool to interpret palaeoenvironmental conditions during deposition and burial and therefore allow discussion about the terranes' relative position. To recognize the magnetic mineral composition and texture of studied Silurian graptolitic shales several rock magnetic measurements were conducted including low-temperature Saturated Isothermal Remanent Magnetization, thermal demagnetization of three-component IRM and hysteresis measurements, as well as anisotropy of magnetic susceptibility (AMS). The sampled rocks come from both units of the HCM. In all analysed samples we found single domain (SD) stoichiometric magnetite of mostly diagenetic (i.e. post-depositional) origin and goethite resulting likely from weathering. In turn, detrital magnetite, even if observed in previously investigated Silurian rocks from the Baltica margin, was not identified in this study, what we attribute to dissolution during diagenesis in the deep-water environment. Solely in the NHCM, SD hematite and maghemite grains were observed, which we interpret as detrital in origin. These grains have been preserved in the suboxic environment of the NHCM sub-basin bottom waters due to their resistance to dissolution in marine waters. Considering the deposition conditions (oxygenation of the near-bottom zone) rather similar for both HCM parts, we associate the presence of aeolian hematite grains solely in the NHCM rocks with a more proximal position of the NHCM than the SHCM in relation to the Baltica continent during late Llandovery (Silurian). This conclusion agrees with some existing palaeogeographic models. In addition to petromagnetic studies focused on the analysis of ferromagnets, AMS measurements were also carried out. The results indicate that the magnetic susceptibility is mainly governed by paramagnetic minerals, mostly phyllosilicates with small ferromagnetic contributions. Oblate AMS ellipsoid and distinct bedding parallel foliation indicate prevailing sedimentary-compactional alignment. Observed magnetic lineation of tectonic origin resulting from weak strain is related presumably to Variscian deformations.

**Key words:** Europe; Magnetic mineralogy and petrology; Rock and mineral magnetism; Sedimentary basin processes; Llandovery (Silurian) mudstones.

## 1 INTRODUCTION

The HCM constitute deformed Cambrian to Carboniferous rocks, covered by Permian to Mesozoic sediments, that were exhumed during Late Cretaceous to Palaeocene, further covered by Miocene marine sediments, and again exhumed in Neogene (Fig. 1; e.g. Lamarche *et al*. 1999, 2003a, b; Mazur *et al*. 2005; Scheck-Wenderoth *et al*. 2008; Krzywiec *et al*. 2009). Generally, the HCM can be divided into two parts, the NHCM, so-called the Łysogóry region, and the SHCM called the Kielce Region, which constitutes the northern margin of the Małopolska Block (Fig. 1). The NHCM and SHCM are separated by the Holy Cross Fault (HCF, Fig. 1, see e.g. Czarnocki 1957, Guterch *et al*. 1984; Mastella & Konon 2002; Konon 2004, 2007; Gągała 2015 for details).

The record of a Silurian period, characterized by biotic and environmental perturbations (e.g. Crampton *et al*. 2016; Trela *et al*. 2016, 2017; Bond & Grasby 2017), is partly preserved in outcrops in both parts of the HCM. Still under consideration is whether both SHCM and NHCM were separated terranes located along the Baltica margin in the Early Paleozoic or they shared in common paleogeographic history before Devonian (e.g. Pożaryski 1990; Lewandowski 1993, 1994; Tomczykowa & Tomczyk 2000; Nawrocki & Poprawa 2006; Poprawa 2006; Nawrocki *et al*. 2007; Kozłowski 2008; Kozłowski *et al*. 2014, Gągała 2015). Nevertheless, in Silurian times, both NHCM and SHCM were located relatively close to the Baltica margin (Torsvik *et al*. 1993, 1996, 2017; Nawrocki *et al*. 2007).

Detailed magnetic studies were investigated to better understand the mechanism of tectonic and sedimentary processes taking place in Silurian. Based on studies such as Karlin and Levi (1983), Karlin (1990), Kars *et al*. (2015) and Niezabitowska *et al*. (2019b), magnetic minerals composition, which provides a piece of information about diagenesis and depositional conditions, was used to verify current geological models of sedimentary basin evolution for both parts of the HCM. Studies were conducted on Silurian graptolitic shales collected from three sites, which are lithostratigraphically uniform for the whole HCM (Fig. 2). To recognize the rock-magnetic properties of analysed shales, comprehensive measurements were performed. Combined results of magnetic anisotropy of analyzed successions and their magnetic mineral composition contributed to determining their origin in the context of the current state of knowledge. The outcome allowed us to infer about the palaeoenvironment, palaeogeography, and burial for both parts of the HCM.

## 2 GEOLOGICAL FRAMEWORK

The HCM is an outcrop of Paleozoic rocks located in central Poland inside the Trans-European Suture Zone (TESZ). Despite numerous studies aimed to decipher the tectonic evolution of the HCM, the tectonic history of docking terranes is still a matter of debate. Generally, the terrane composition of the HCM is a result of subsequent orogenic processes from Cadomian to Variscian, while the association of the terranes reached the nearby present Baltica position in Silurian (Pożaryski 1991; Belka *et al*. 2000, 2002; Cocks 2002; Torsvik & Rehnström 2003; Cocks & Torsvik 2005; Nawrocki & Poprawa 2006, Nawrocki *et al*. 2007; Verniers *et al*. 2008). Decoupled tectonic evolution of the NHCM and SHCM during Caledonian orogeny is reflected in lithostratigraphic contrast between nearly continuous late Silurian - Early Devonian sedimentary succession in the NHCM and well-preserved base-Emsian (Caledonian) unconformity in the SHCM (e.g. Czarnocki 1950; Mizerski 1979; Narkiewicz *et al*. 2006; Kozłowski 2008; Kozłowski *et al*. 2014). However, Kozłowski *et al*. (2004) and Kozłowski (2008) proposed that the Silurian sediments of both parts of the HCM were deposited in one continuous sedimentary basin on the southwestern passive margin of Baltica, where sediments from western NHCM have a more proximal position to the land.

During Ordovician and Silurian times, the sedimentation regime in the HCM was determined by the approaching Caledonian orogen, which extended along a collision zone of the southern margin of Baltica with a subductive island arc, the Eastern Avalonia terrane and other peri-Gondwana terranes (Jaworowski 2000; Poprawa 2006). The progressive docking of the terrane led to the formation of an orogenic wedge with a foredeep basin, where the subsidence was determined by the flexural bending of the Baltica margin (e.g. Poprawa *et al*. 1999; Poprawa *et al*. 2010). The continuous infill of a foreland basin is preserved in the NHCM (Czarnocki 1950; Mizerski 1979). Therefore, the lower Paleozoic tectonic evolution is reflected by the sedimentary strata of the NHCM. Corresponding, but less complete succession, laying unconformable on the Cambrian, is preserved in the SHCM (see Fig. 2; e.g. Filonowicz 1971; Narkiewicz 2002; Kozłowski 2008).

### 2.1. Sedimentation deposition and depth of the Silurian basin in the HCM

The Silurian section of HCM, from both NHCM and SHCM, represents unmethamorphosed, moderately folded layers of epicratonic deposits (e.g. Mizerski 2004; Kozłowski 2008). The Silurian sediments are formed by two main successions (Fig. 2). First one was deposited on the continental deep shelf of Baltica and the graptolitic shales sequence was developed from Llandovery to lower Ludlovian, whereas the upper part of Silurian rocks consists of early Ludfordian graywackes (e.g. Tomczykowa & Tomczyk 1981). In the central part of NHCM, the Silurian section's upper part (Pridoli) also comprises carbonates, which pass continuously into Lower Devonian siliciclastic (e.g. Czarnocki 1950; Tomczyk *et al*. 1977; Kozłowski 2008).

Clastic deep shelf sedimentation of graptolitic shales, according to Jaworowski (1971) and Kozłowski (2008), was present continuously in one large foreland sedimentary basin on the southwestern margin of the Baltica continent, however, the sediments layer in the NHCM is thicker (Fig. 2). The approaching Caledonian orogen was a source of clastic material and resulted in intense greywacke sedimentation causing infilling of the basin and appearing of the clastic wedge during early Ludlow (Narkiewicz 2002; Kozłowski *et al*. 2004). Afterward, the sedimentation environment changed into a clastic-carbonate shallow shelf in an intense subsidence regime (e.g. Kozłowski 2003). The later sedimentation in the NHCM is followed by a thick layer of the mainly clastic succession of sediments representing continuous infilling of the foreland basin from Ludlow (Silurian) to Lochkovian (Lower Devonian; e.g. Narkiewicz 2002; Kozłowski 2008). Similarly, in the SHCM the sedimentation of dark graptolitic shales deposited in progressive oxygen deficiency related to the deepening of the sea during the uppermost Ordovician–lowermost Silurian (Masiak *et al*. 2003) was rapidly replaced by medium- to coarse-grained greywackes with conglomerates in early Ludlow (Tomczyk 1970). In contrast to the NHCM, in the SHCM the lower Paleozoic units are unconformably covered

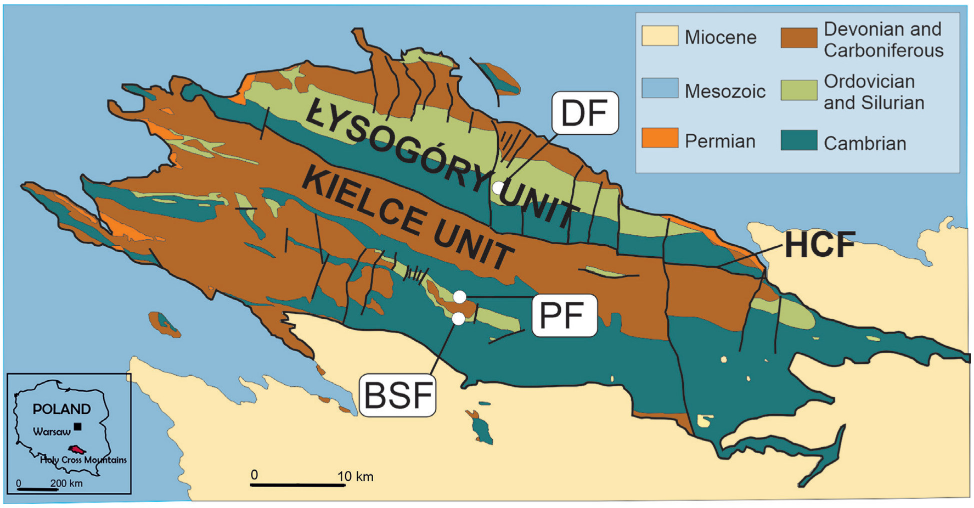


**Figure 1.** Simplified geological map of the Holy Cross Mountains (after Czarnocki 1957, modified) with marked location of the sampled sites. Abbreviations: DF, the Dębniak Formation; PF, the Prągowiec Formation; BSF, the Bardo Stawy Formation; HCF, the Holy Cross Fault.

by Emsian (Devonian) sediments (Bednarczyk *et al*. 1970; Kowalczewski 1971; Głazek *et al*. 1981; Tarnowska 1981; Malec 1993; Szulczewski 1995).

An important element that influenced the sedimentation system in Ordovician and Silurian in the HCM was the eustatic factor (e.g. Kozłowski 2003, 2008; Masiak *et al*. 2003). After the Hirnantian (Ordovician) glacial maximum caused by Gondwana glaciation, the series of transgressions occurred in Llandovery (Silurian), including late Rhuddanian and middle Aeronian high-stands (Fig. 2; after e.g. Witzke 1992; Johnson, 1996, 2006, 2010; Davies *et al*. 2016), reaching the maximum rise in late Telychian (Llandovery, Silurian; after Johnson *et al*., 1998). Then, slowly decreased until early Gorstian (Ludlow) with one exception in Sheinwoodian (Wenlock), where an increase was observed (Fig. 2, after Johnson 1996; Johnson *et al*. 1998).

In Silurian, when Baltica drifted to the tropical realm (Torsvik *et al*. 1993, 1996, 2017), several global sedimentary events affecting taxa took place (e.g. Johnson *et al*. 1998; Jeppsson & Calner 2002). In the analysed time interval, the most significant and well-recognized were the Ireviken Event, which spans the Llandovery–Wenlock boundary (e.g. Johnson *et al*. 1998) and Mulde Event extending over late Wenlock to early Ludlow (e.g. Jeppsson & Calner 2002). Both events, affecting primarily hemipelagic and pelagic organisms, were caused by expanding suboxic/anoxic conditions of bottom waters and fluctuating salinity associated with deglaciation (Smolarek *et al*. 2017).

### 2.2 Material—lithology, thickness and sedimentation conditions

Only a few natural outcrops of Ordovician and Silurian rocks are or were present recently in the HCM area. Especially in the NHCM, there are no natural outcrops nowadays and it is worth noting that previous studies were based on drill cores material (e.g. Smolarek *et al*. 2014, Trela *et al*. 2016, 2017). Here, for study purposes, we decided to perform an excavation. In turn, in the SHCM among identified outcrops, the Bardo Syncline Silurian deposits are preserved the best (Fig. 2). The sampled Bardo Stawy outcrop is currently the only place in the HCM area, where a continuous sedimentary profile and the contact between lower Silurian shales and upper Ordovician mudstones can be observed (see e.g. Trela & Salwa 2007 for details).

Analyzed samples were collected from three sites located in the NHCM and the SHCM (Figs 1 and 2). From the NHCM the material was taken from an informal lithostratigraphic unit called the Dębniak Beds (Tomczyk 1962; Deczkowski & Tomczyk 1969) from an excavation carried out. In turn, from the SHCM two natural outcrops were exploited in the area of the Bardo Syncline, including (1) the Prągowiec Beds from the Prągowiec Ravine from the northern limb and (2) black shales of the Zbrza Member, which belongs to the Bardo Stawy Formation from the southern limb (Fig. 2; Trela & Salwa 2007).

Grey to greenish-grey claystone to clayey graptolitic mudstones of the Dębniak Beds are assigned to the upper Llandovery (Aeronian–Telychian) with a thickness of 30–40 m (e.g. Modliński & Szymański 2001). Sampled dark/black and grey shales of the Dębniak Beds, during early Aeronian and early Telychian, were deposited in anoxic to dysoxic conditions, and thus show elevated TOC values. These horizons are a record of post-glacial transgressions (Trela *et al*. 2016). The main Llandovery lithofacies (upper Aronian and middle to upper Telychian parts), represented by greenish-grey mudstones, were formed in more oxygen-enriched conditions caused by deep-water ventilation and benthic oxygenation during regressive periods, where some intervals display subtle bioturbation mottling and rare evidence of bottom current activity was found (Trela *et al*. 2016). However, these homogenous mudstones are interrupted by the dark to black shale interbeds and laminae (Trela *et al*. 2016). In contrast to the eastern margin of the NHCM, in the sampled central part, continuous sedimentary deposition across the Ordovician and Silurian boundary is observed (Tomczyk 1962; Deczkowski & Tomczyk 1969; Trela *et al*. 2015, 2016).

The 600-m-long Prągowiec Ravine is represented by a 150-m-thick profile of lower Ludlovian- upper Wenlockian yellowish- to greenish-grey and dark grey clayey shales, called Prągowiec Beds (Tomczykowa 1958; Tomczykowa & Tomczyk 1981) and above them, lower Ludlovian greywacke sediments of the Niewachlów Beds (Malec *et al*. 2016). The analysed Prągowiec section constitutes shales with graptolites and very rare benthic fauna abundance (Tomczykowa 1958), deposited in the deep pelagic environment, which generated temporary anoxic conditions at the bottom

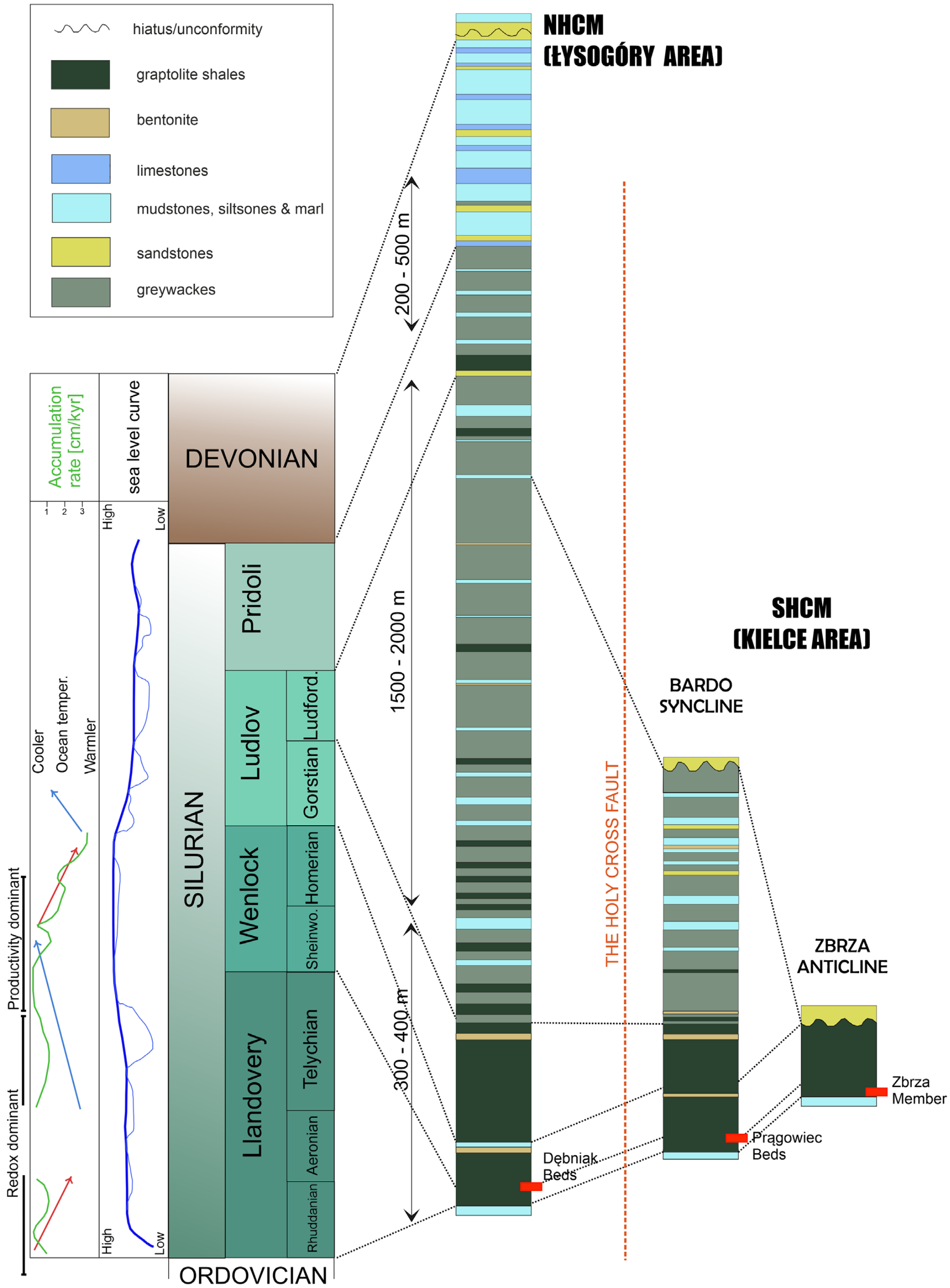


**Figure 2.** Simplified lithostratigraphic profile of Silurian sediments of the Holy Cross Mountains (modified after Filonowicz 1971; Kozłowski 2008). The northern (NHCM) and southern (SHCM) parts are divided by the Holy Cross Fault (red line). The samples were collected from the graptolite shale formations from both parts of the HCM, marked here as red rectangles. The sea level curve for Baltica from Johnson (1996), while the other data, including accumulation rate, ocean temperature, and productivity-preservation states come from Hunslow *et al*. (2021).

(Kozłowski *et al*. 2004; Radzevičius *et al*. 2019). In turn, the upper greywacke sandstones with mudstone interbeds were deposited by turbidity currents from the southwest (Malec *et al*. 2016). These rocks are composed mostly of volcanic and sedimentary lithoclasts as well as metamorphic and rare plutonic lithoclasts, which were transported from the Caledonian orogen and the continental volcanic arc (Malec *et al*. 2016).

The Bardo Stawy outcrop characterizes a continuous lithological profile from Hirnantian (Ordovician) Zalesie Formation mudstones through the lower Llandovery (Rhuddanian, Silurian) Bardo Formation. The Bardo Formation is represented by black radiolarian cherts, called the Rembów Member, changing upwards into graptolitic shales, named Zbrza Member (Trela & Salwa 2007). These rocks are explained as transgressive to highstand deposits formed in marine flooding environments starting in the Late Ordovician (Trela & Salwa 2007). In more detail, the radiolarian cherts overlaying on mudstones were formed in decreasing thermohaline circulation and increasing transgression environment, which together with upwelling, impacted higher primal organic matter production and developed dysoxic to anaerobic conditions in relatively shallow shelf seas (Kremer 2005; Trela *et al.* 2006; Trela & Salwa 2007). In turn, graptolitic shales of Zbrza Member were deposited in a highstand and stable environment with temporally increasing oxygenation in the water column, deduced from bioturbations (Trela & Salwa 2007).

In summary, the studied rocks from the NHCM and SHCM, characterize deposition conditions influenced by the global palaeoceanographic conditions variations in the early Silurian times. These are defined by benthic oxygen increase caused by an intensive thermohaline circulation while glacial maxima and regressions, which were interrupted, however, by anoxic transgressive events (Page *et al.* 2007; Trela *et al.* 2016). Specifically, graptolitic shales/mudstones were deposited in largely upper to lower dysoxic conditions, which were influenced seasonally by oxygenation of bottom waters in the NHCM part (see e.g. Trela *et al.* 2016; Smolarek *et al.* 2016 for more details). Sampled rocks are characterized by elevated TOC values (2 up to 8 per cent) on the O/S boundary for the Zbrza Member in the Bardo Stawy site (SHCM, after Smolarek *et al.* 2017), whereas the lower TOC values (0.39 and 1.71 per cent) for the Dębniak Beds (after Trela *et al.* 2016). No turbidity currents were observed in sampled shales from both parts of the HCM.

### 2.3 Thermal evolution of the HCM

The role of burial influencing Paleozoic (post-Cambrian) sediments is still a matter of debate and several contradicting models of thermal evolution have been proposed based on color alteration indexes of Palaeozoic microfossils, apatite and zircon thermochronology, or vitrinite and graptolite reflectance data (e.g. Smolarek-Lach *et al.* 2014; Schito *et al.* 2017; Botor *et al.* 2018). Generally, most of the studies suggest that the main thermal event was the Varisican (lower Carboniferous to early Permian, e.g. Bełka 1990; Marynowski 1999; Marynowski *et al.* 2002; Narkiewicz *et al.* 2010; Smolarek *et al.* 2014; Naglik *et al.* 2016; Narkiewicz 2017). However, it has been proposed that also during the Mesozoic the temperature substantially increased across most of the HCM, which was caused by subsidence and resulting burial (e.g. Poprawa *et al.* 2005; Botor *et al.* 2018). Final cooling was caused by tectonic inversion during Upper Cretaceous (Krzywiec 2002; Lamarche *et al.* 2003a, b; Scheck-Wenderoth *et al.* 2008).

Thermal maturation differs between the NHCM and SHCM (e.g. Szczepanik 1997, 2007; Malec 2000; Narkiewicz 2002; Smolarek *et al.* 2014). The NHCM shows highly altered organic matter and thermal maturation from mid-mature to over-mature, whereas immature to late mature for the SHCM (e.g. Smolarek *et al.* 2014; Schito *et al.* 2017). Generally, the maturation increases towards the HCF for both parts of the HCM (after Szczepanik 2007; Narkiewicz 2002). Malec (2000) proposed that the NW part of the SHCM has similar burial evolution to the NHCM, which was later confirmed by studies by Narkiewicz (2002). Nevertheless, the whole HCM area experienced maximal burial temperatures above 100 °C (Bełka 1990; Barker & Pawlewicz 1994; Marynowski 1999; Marynowski *et al.* 2001; Narkiewicz *et al.* 2010; Środoń & Trela 2012; Smolarek *et al.* 2014; Schito *et al.* 2017). According to Marynowski *et al.* (2001) and Schito *et al.* (2017), the Dębniak greywackes and mudstones (Ludlow) show maximal temperatures around 170–200 °C. In turn, the SHCM bentonites from Pragowiec (Ludlow) and Bardo (Wenlock) experienced temperatures around 100–110 °C (Marynowski *et al.* 2001; Smolarek *et al.* 2014; Schito *et al.* 2017).

## 3 METHODS

### 3.1. Room and high-temperature rock magnetic methods

The experiments were performed at the Palaeomagnetic Laboratory of the Institute of Geophysics, Polish Academy of Sciences, Warsaw, Poland. The measurements were initiated on 14 cylindrical specimens with the acquisition of isothermal remanent magnetization (IRM using an MMPM1 pulse magnetizer and a 2 G SQUID cryogenic magnetometer in a shielded room (noise level: ~$10^{-10}$ $Am^2$). Standard specimens 26 × 22 mm in size were prepared for analysis purposes. The Maxbauer *et al.* (2016) statistical method was applied to decompose the magnetization curves by the MAX UnMix web application. The hysteresis loops were analyzed using a MicroMag AGM vibration magnetometer (noise level: ~$10^{-7}$ $Am^2$). A total of 91 specimens, the chips of rock weighing approximately 20 mg, were demagnetized before the measurements. The default (70 per cent) setting of the dia/paramagnetic adjustment was applied for the slope correction. The ferromagnetic/paramagnetic content was calculated from the initial slope before and after correction for paramagnetic minerals.

To better establish magnetic mineral composition thermal demagnetization of three-component IRM (after Lowrie, 1990) was carried out using a 2 G SQUID cryogenic magnetometer and a Magnetic Measurements MMTD-80 thermal demagnetizer. Eight specimens were magnetized in three orthogonal axes applying 0.15, 0.5 and 4 T field with MMPM1 pulse magnetizer and thermally demagnetized in 24 steps to reach 700 °C. To estimate the para- and ferromagnetic contribution of the magnetic minerals temperature variation of magnetic susceptibility was monitored by Kappabridge KLY-3S of Agico (sensitivity: $2 \times 10^{-8}$ [SI], accuracy: 0.3 per cent) in an air atmosphere. The method of Hrouda (1994) and Hrouda *et al.* (1997) was applied to fit the hyperbola using the least-squares method to the initial part of the curve ranging from 50 to 250 °C. Additionally, two samples from both NHCM and SHCM were measured in an argon atmosphere in a sequence divided into two steps of warming and cooling (1) up to 400 °C and (2) up to 700 °C.

The low-field anisotropy of magnetic susceptibility (AMS) measurements were performed on 71 cylindrical specimens with a Multifunction KappaBridge MFK1-FA (sensitivity $2 \times 10^{-8}$ [SI]) by AGICO Instruments (Jelínek & Pokorný 1997). The AMS was measured in a 200 A $m^{-1}$ field at room temperature. Basic AMS parameters were calculated using the Anisoft software of AGICO. Three orthogonal axes, K1, K2 and K3—maximum, intermediate and minimum, forming the ellipsoid of magnetic susceptibility and magnetic fabrics, were defined. These factors are identified by several parameters like the degree of anisotropy (P), defined as K1/K3, the magnetic lineation (L), expressed as K1/K2 and the magnetic foliation (F), calculated as K2/K3 (Hrouda 1982).

### 3.2. Low-temperature remanence

The measurements in low temperatures were performed at the Institute for Rock Magnetism, University of Minnesota in Minneapolis, USA, using Magnetic Properties Measurement System instruments (MPMSs, Quantum Design INC., San Diego). All measurements were conducted on thirteen powder specimens of about 400 mg sealed in gel capsules.

The measurement procedure starts with applying a 2.5 T field to reach Saturated Isothermal Remanent Magnetization (SIRM). The next step is to cool down a specimen from temperature 300 to 10 K (from 26.85 to –263.15 °C) in a very weak magnetic field (+5 µT) in 5 K steps. This measurement is called Room Temperature SIRM (RT-SIRM). However, as a measurement of remanence, SIRM is performed without a magnetic field, here the application of a 5 μT field allows to intensify of the effect of paramagnetic minerals occurrence, the so-called P-behavior investigated by Kars *et al*. (2014, 2015). The procedure was initially proposed as an indicator of nano-pyrrhotite (see Aubourg & Pozzi 2010). The next part of the measurement sequence was to apply a 2.5 T field at 10 K (–263.15 °C) to reach LT-SIRM (Low-Temperature SIRM). After switching off the field, a specimen was warmed up to 300 K (26.85 °C) in Zero Field (ZF) in 10 K steps. To obtain further details on grain size [stable single domain (SSD) versus multidomain (MD)], as well as genesis (organic versus inorganic) along with the sequence some specimens have additional steps performed. Moskowitz *et al*. (1993) and then, for example Carter-Stiglitz *et al*. (2004) suggested that measurement of LTRM on warming (typically 20–300 K) from two initial states - zero-field cooled (ZFC, prior to the application of a 2.5 T), and field cooled (FC, in 2.5 T field)—provides a diagnostic signature of the presence of chains of SSD magnetite (magnetosomes) produced by magnetotactic bacteria. Thus, a more comprehensive measurement sequence comprises two previous steps: Field Cooling (FC), which is a measurement of magnetization in a continuous 2.5 T induced field during cooling, and Zero Field Cooling (ZFC), which is a measurement of magnetization in zero magnetic fields. Moreover, selected specimens were first heated to 400 K (126.85 °C) to remove the goethite contribution (if any occur) by heating through the Néel temperature of goethite [393 K (120 °C) Özdemir & Dunlop 1996].

## 4 RESULTS

### 4.1. Results of high and room temperature rock magnetic measurements

The thermal variation of magnetic susceptibility studies exhibits similar results for both parts of the HCM. The initial part of the curves displays a hyperbolic to flat shape that is characteristic of the presence of paramagnetic and ferromagnetic minerals, respectively (Figs 3a, b and c). In the Dębniak Beds (Fig. 3c), the heating curve displays an increase in susceptibility at around 300 °C, followed by a noticeable hump. This increase might be due to the production during the heating of maghemite from some less magnetic Fe-hydroxides (after Oches & Banerjee 1996). The increase of susceptibility appears at temperatures over 400 °C in samples representing the SHCM part, both in air and argon atmosphere (Figs 3a, b and d). The thermochemical changes are likely related to the formation of new magnetite, as the final product has a Curie temperature of around 580 °C. The significantly enhanced susceptibility after thermal treatment is attributed to the transformation of iron sulfides and iron-containing silicates/clays to a new ferrimagnetic mineral phase during heating (e.g. Hunt *et al*. 1995). Note, there was no lambda transition observed in the 225–245 °C temperature range indicative of the presence of pyrrhotite (see Schwarz 1975). The separation method for distinguishing the ferromagnetic from the paramagnetic components indicates that the Ferro/para ratio usually is in the 3–15 per cent range.

The outcome from the ‘ferro-para’ separation method is in line with the hysteresis analysis. The hysteresis parameters show the dominant contribution of paramagnetic minerals in magnetization values, with a small to modest impact on the ferromagnetic phase (Figs 4a and b). It changes from 7 to 9 per cent at the NHCM (the Prągowiec Beds) and in the southern part of the SHCM, but in the northern part of the SHCM (the Zbrza Member), the value reaches 38 per cent (Table 1). In general, hysteresis parameters are consistent within the formation, however, an exception constitutes the Prągowiec Beds, where Ms values vary from 546 to 5786 $\mu Am^2 kg^{-1}$. The values of Ms and Mr and quite similar for the Prągowiec and Dębniak beds, while for the black shales of the Zbrza Member, lower values of Ms and higher values of Mr were observed (Table 1, Figs 4a and b).

Results of thermal demagnetization of the IRM components for the Dębniak samples show a significant contribution of both low and high-coercivity minerals (Fig. 4c). The losses of magnetization on a low coercivity curve observed around 570 °C suggest the occurrence of magnetite, while the final drop of magnetization above 600 °C can be interpreted as the presence of maghemite (Fig. 4c). In turn, from a high coercivity curve, two different magnetic minerals can be identified: (1) goethite, related to unblocking temperature around 100 °C and (2) hematite, due to the final loss of magnetization at 680 °C (Fig. 4c). The slight impact of medium coercivity minerals is detectable, a visible drop in temperature at 625 °C, suggests the presence of maghemite. Moreover, decreasing remanence in the range of 300–330 °C, we attribute to the presence of iron sulfides (Fig. 4c). The disruptions are associated with thermochemical alterations.

The results of the IRM acquisition for both parts of the HCM show a fast increase of the remanence below 0.5 T repeatable in each specimen, suggesting a significant amount of low and medium coercivity minerals (Fig. 5a). Further, a continuous increase of the remanence between 0.5 and 4 T indicates the presence of high coercivity minerals like hematite and goethite. Decomposition of the IRM data using MAX UnMix (after Maxbauer *et al*. 2016) reveals two magnetic components in the SHCM (Figs 5c and d), and three in the NHCM (Fig. 5b). The low coercivity component (component 1) in the SHCM is characterized by a $B_h$ (the mean coercivity of an individual grain population, after Maxbauer *et al*. 2016) of 1.32 (±0.02) log10 units (20.9 mT), and the dispersion parameter (*DP*) of 0.67 (±0.06; see Fig. 5c). Component 2 has a $B_h$ of 3.55 (±0.05) log10 units (3.56 T) and a DP of 0.29 (±0.03; see Fig. 5c). In turn, for the NHCM part, the low coercivity component is defined by a $B_h$ of 1.65 (±0.02) log10 units (45.5 mT) and a *DP* of 0.4 (±0.01; see Fig. 5b), while high coercivity component (component 2) has a $B_h$ of 3.48 (±0.03) log10 units (3.01T) and *DP* of 0.33 (±0.02). Here, in contrast to the SHCM, another high coercivity mineral was observed (component 3), which has a $B_h$ of 2.56 (±0.06) log10 units (366 mT) and *DP* of 0.27 (±0.06). This component (3) is interpreted to represent fine-grained hematite (or oxidized magnetite). For both parts of the HCM, the low coercivity component (component 1) was identified as magnetite, while the high coercivity component (2) was attributed to goethite.

### 4.2. Results of low-temperature remanence

The Dębniak Beds samples display a well-developed Verwey transition on RT-SIRM curves (Fig. 6c). However, in both ZFC and FC curves the transition is hardly visible (Fig. 6a), which may suggest titanium substitution or a grain size effect (for further discussion see Section 5.1.). The transition occurs at ~110-115 K [–163.15 to (–158.15) °C], which suggests a small degree of cation deficiency, probably modified by maghemitization (after Özdemir *et al*. 1993). FC SIRM has a higher intensity than a ZFC low-T SIRM suggesting single domain (SD) magnetite (Moskowitz *et al*. 1993). The

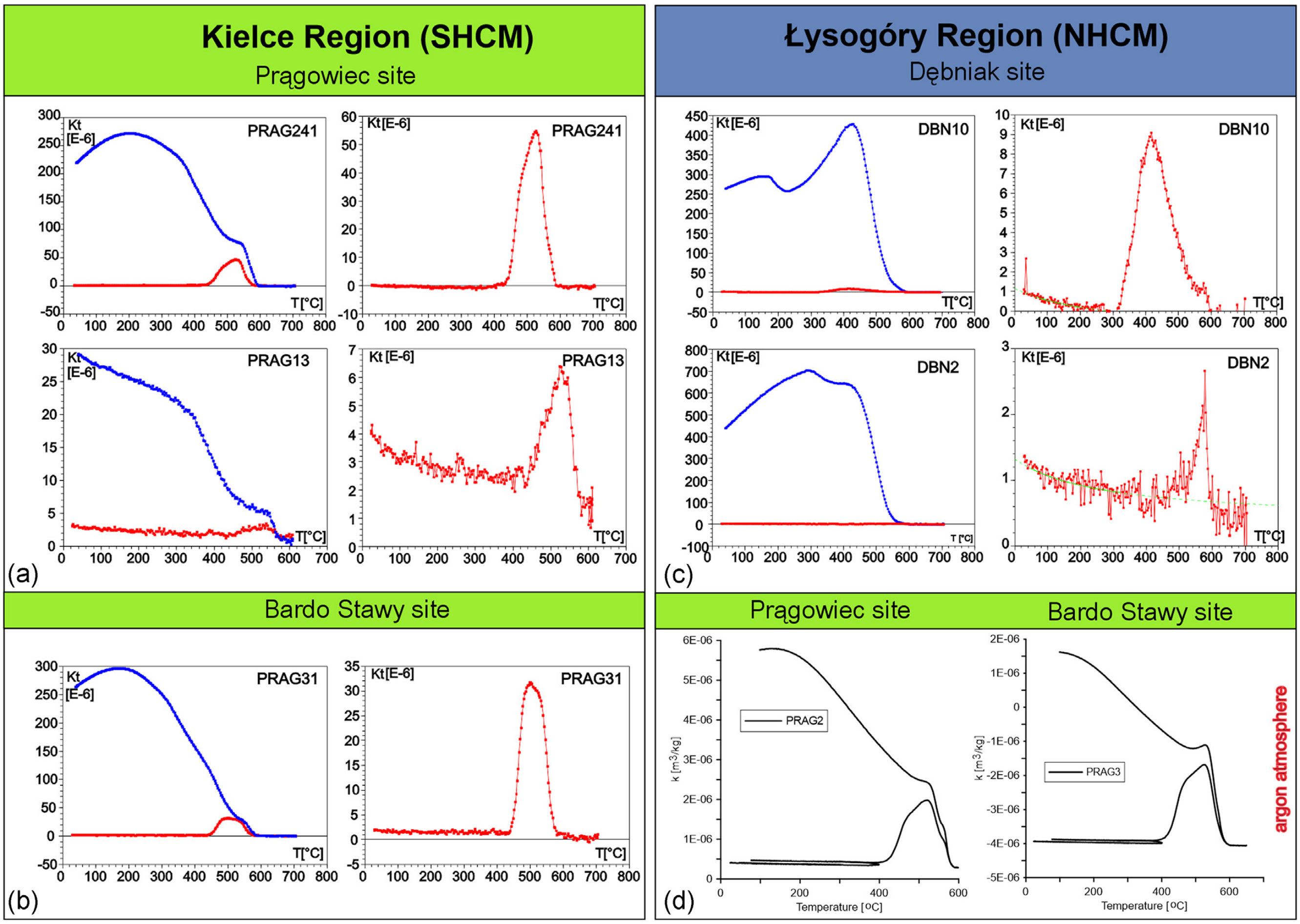


**Figure 3.** Temperature dependence of magnetic susceptibility in air atmosphere of selected specimens of graptolitic shales from the Kielce Region (SHCM) from two sites (a) the Prągowiec and (b) the Bardo Stawy site (Zbrza Member samples), and from the Dębniak site from the Łysogóry Region (c, the NHCM), while heating (red) and cooling (blue curves); (d) temperature dependence of magnetic susceptibility in argon atmosphere for representative samples from the NHCM part, from Prągowiec and Bardo Stawy sites.

RT-SIRM curves present a decrease of remanence during warming to 400 K (126.85 °C) indicative of reaching the Néel temperature ($T_N$) characteristic for goethite (Fig. 6b; see Özdemir & Dunlop 1996). Higher values of FC than ZFC remanence curve and increasing differences between them while cooling confirm the occurrence of goethite grains (Fig. 6B; after Özdemir and Dunlop, 1996; Liu *et al*., 2006). Moreover, small humps of the curves around 200 K (–73.15 °C) are indicative of the presence of hematite (Figs 6b and c). The Besnus transition, characterized by an increase in Mrs, Bc and Bcr on cooling through the 34–28 K range, which implies the presence of pyrrhotite (e.g. Fillion & Rochette 1988; Dekkers *et al*. 1989; Volk *et al*. 2016), was not observed in the analysed data.

Similar results were obtained for samples collected from the SHCM. For both sites the results are consistent, on RT-SIRM curves the Verwey transition is well developed at 115–120 K [−158.15 to −153.15 °C], slightly below the transition temperature for pure stoichiometric magnetite (Figs 6f and k). These values and the differential shape of ZFC curves (Figs 6e and h) suggest a small degree of cation deficiency. Similarly like in the Dębniak Beds (NHCM), the transition is not marked on FC or ZFC curves. Significantly higher values of FC magnetization than ZFC and an increase of the remanence during cooling from 300 to 50 K (−263.15 to 66.85 °C) suggest the presence of goethite (Figs 6d and g). Contrary to the NHCM, no sign of hematite is visible.

Generally, in all specimens, ZFC and FC remanences gradually decrease with increasing temperature with no distinct drops (Figs 6a, d and g), which may indicate the presence of magnetite, hematite, pyrrhotite, siderite or rhodochrosite (e.g. Passier & Dekkers, 2002, see Section 5.1. for further discussion). An exception constitutes the ZFC curve for the Prag3_hcm specimen, where approximately 50–60 per cent losses of magnetization upon warming to 35 K (−238.15 °C, Fig. 6h) are observed. The rapid decrease of remanence may suggest (a) unblocking of very small superparamagnetic (SP) or SD particles and/or (b) decreasing magnetocrystalline anisotropy in phases like goethite (e.g. Banerjee *et al*. 1993; Passier & Dekkers 2002).

### 4.3. Low-field anisotropy of magnetic susceptibility

Magnetic susceptibility of the Dębniak mudstones varies between 137 and 180 × $10^{-6}$ (SI), similar to the Zbrza Member (160–195 × $10^{-6}$), while in the Prągowiec values are somewhat lower and do not exceed 129 × $10^{-6}$ (Fig. 7d). The shape of the AMS ellipsoid for the Dębniak mudstones is strongly oblate, which is consistent with the results for the Zbrza Member (Figs 7a, c and d). In turn, in the Prągowiec Beds shape of AMS ellipsoids are more differential and varies from predominantly oblate to triaxial (Figs 7b and d). The

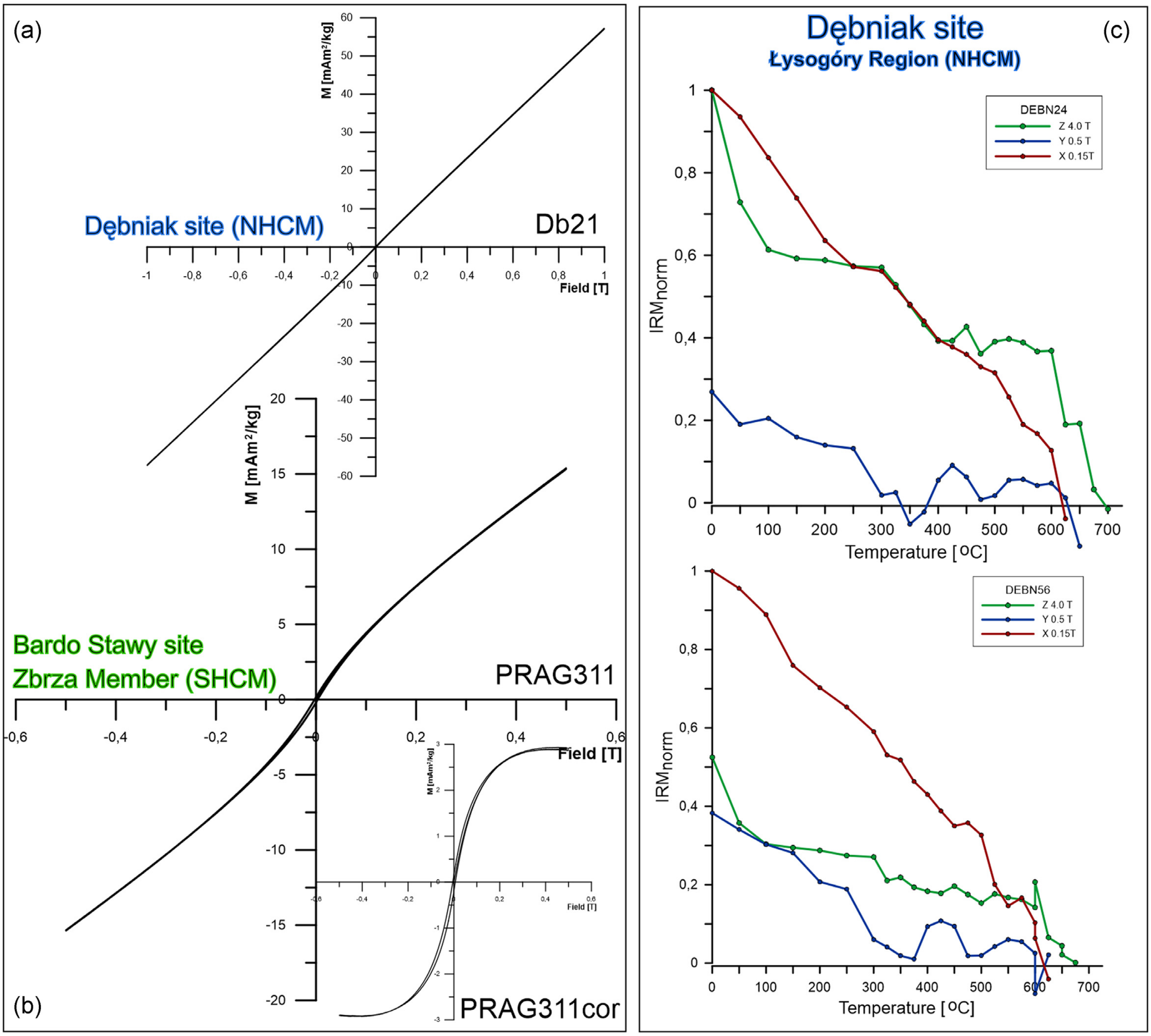


**Figure 4.** Results of hysteresis loops for selected specimens from the Dębniak Beds (a) and from the Bardo Stawy site from the Zbrza Member (b), before and after correction for paramagnetic contribution. (c) Thermal demagnetization of three-component IRM (0.15, 0.5 and 4 T) for selected specimens from the Dębniak Beds.

degree of anisotropy (*P*) is consistent, for the Dębniak and Zbrza Member beds and reaches around 1.035 and 1.056, respectively. In Prągowiec shales values of the *P* parameter are in the 1.020–1.043 range (Fig. 7d).

The degree of mean foliation (*F*) reaches even 1.054 for the Zbrza Member and 1.045 for the Dębniak Beds, while for the Prągowiec it is the lowest with the average value of 1.021 (Fig. 7d). Magnetic foliation is bedding parallel in all sites. Minimal axes are well grouped in Prągowiec formation and Zbrza Member, either their distribution shows some NNE-SSW elongation for the Dębniak mudstones (Figs 7a, b and c). The magnetic lineation (*L*) observed in mudstones is relatively weak (here the average *L* parameter for specimens is below 1.006), however, it is well notable for all sites (Fig. 7d). In the Prągowiec and Zbrza sites, the maximal AMS axes are distributed in the bedding plane showing some tendency to WNW–ESE grouping. In turn, maximal AMS axes in the Zbrza Member are very well clustered in the same WNW–ESE orientation.

## 5 DISCUSSION

### 5.1 Magnetic mineral composition

#### *5.1.1 Magnetite and goethite*

The results document the occurrence of magnetite and goethite in all analyzed specimens. The Verwey transition below 120 K, suggests the presence of nearly stoichiometric magnetite (e.g. Özdemir *et al*. 1993; Carter-Stiglitz *et al*. 2004). In each sample, the observed transition is not sharp, but spread out over twenty degrees (or more) temperature range. A variety of factors can explain the suppression of the Verwey transition such as cation substitution and/or non-stoichiometry of magnetite or grain size effect (e.g. Syono 1965; Aragón *et al*. 1985; Kąkol & Honig 1989; Kąkol *et al*. 1992; Moskowitz *et al*. 1993; Özdemir *et al*. 1993; Halgedahl & Jarrard 1995; Moskowitz *et al*. 1998). However, in analysed samples in the ZFC/FC curves demagnetization of the goethite phase

**Table 1.** The parameters from hysteresis loops analysis for samples from the Kielce (SHCM, green colour) and Łysogóry Region (NHCM, blue colour), with the mean values per each parameter per site calculated. The ferromagnetic/paramagnetic content was calculated from the initial slope before and after correction for paramagnetic minerals. Ms – Saturation Magnetization after correction for paramagnetic minerals at 400 mT, Mr - magnetic remanence, Bc – coercivity.

| Region | Site | Sample | Ms [$\mu Am^2 kg^{-1}$] | Mr [$\mu Am^2 kg^{-1}$] | Bc [mT] | Ferro/para content [per cent] | Region | Site | Sample | Ms [$\mu Am^2 kg^{-1}$] | Mr [$\mu Am^2 kg^{-1}$] | Bc [mT] | Ferro/para content [per cent] |
|---|---|---|---|---|---|---|---|---|---|---|---|---|---|
| KIELCE REGION (SHCM) | Prągowiec Beds | Prag_11 | 802 | 31.4 | 4.3 | 6.5 | KIELCE REGION (SHCM) | Bardo Stawy site (Zbrza Member) | Prag_311 | 2881 | 174.8 | 5.6 | 48.1 |
| | | Prag_12 | 3542 | 72.1 | 3.5 | 21.4 | | | Prag_312 | 1494 | 29.8 | 1.7 | 34.6 |
| | | Prag_13 | 1245 | 55.3 | 4.5 | 9.3 | | | Prag_321 | 1423 | 30.7 | 1.8 | 32.2 |
| | | Prag_14 | 1091 | 58.8 | 7.2 | 3.7 | | | Prag_322 | 2392 | 113.2 | 4.0 | 42.5 |
| | | Prag_15 | 911 | 53.4 | 6.4 | 7.4 | | | Prag_331 | 1179 | 48.7 | 3.5 | 38.7 |
| | | Prag_16 | 803 | 76.2 | 7.8 | 8.6 | | | Prag_332 | 1813 | 100.9 | 4.6 | 38.2 |
| | | Prag_17 | 643 | 33.9 | 5.1 | 7.0 | | | Prag_3581 | 1712 | 65.6 | 3.1 | 39.9 |
| | | Prag_18 | 1291 | 63.8 | 4.3 | 8.8 | | | Prag_3671 | 1593 | 52.7 | 2.6 | 41.9 |
| | | Prag_19 | 1206 | 55.8 | 5.1 | 8.8 | | | Prag_3672 | 1797 | 50.6 | 2.4 | 46.2 |
| | | Prag_110 | 1579 | 52.8 | 3.7 | 14.8 | | | Prag_3711 | 1521 | 58.2 | 3.1 | 34.1 |
| | | Prag_111 | 699 | 20.2 | 4.4 | 7.6 | | | Prag_3712 | 1735 | 68.6 | 3.2 | 38.9 |
| | | Prag_112 | 963 | 40.1 | 5.1 | 7.1 | | | Prag_341 | 1331 | 33.1 | 2.1 | 29.9 |
| | | Prag_113 | 975 | 49.2 | 5.4 | 8.2 | | | Prag_342 | 1351 | 59.7 | 3.5 | 30.3 |
| | | Prag_114 | 1037 | 78.8 | 7.3 | 9.3 | mean values | | | 1709.4 | 68.2 | 3.2 | 38.1 |
| | | Prag_115 | 856 | 44.3 | 6.0 | 6.9 | ŁYSOGÓRY REGION (NHCM) | Dębniak Beds | Debn21 | 684 | 23.0 | 3.0 | 7.3 |
| | | Prag_116 | 668 | 46.4 | 6.5 | 9.0 | | | Debn31 | 617 | 8.2 | 2.2 | 4.6 |
| | | Prag_117 | 875 | 56.3 | 5.3 | 7.7 | | | Debn41 | 495 | 2.8 | 1.7 | 5.1 |
| | | Prag_118 | 796 | 52.6 | 5.2 | 7.6 | | | Debn71 | 558 | 3.1 | 1.6 | 5.9 |
| | | Prag_211 | 1147 | 68.4 | 6.8 | 8.1 | | | Debn81 | 625 | 13.0 | 3.3 | 5.8 |
| | | Prag_231 | 919 | 64.6 | 7.5 | 8.3 | | | Debn91 | 1222 | 52.2 | 6.0 | 9.2 |
| | | Prag_241 | 759 | 59.4 | 7.7 | 7.0 | | | Debn101 | 1352 | 5.2 | 1.3 | 10.5 |
| | | Prag_251 | 945 | 52.2 | 6.3 | 9.1 | Mean values | | | 793.2 | 15.4 | 2.7 | 6.9 |
| | | Prag_261 | 855 | 49.8 | 6.5 | 8.1 | | | | | | | |
| | | Prag_271 | 635 | 45.1 | 6.5 | 7.1 | | | | | | | |
| | | Prag_281 | 917 | 57.9 | 6.4 | 8.9 | | | | | | | |
| | | Prag_212 | 5689 | 48.2 | 6.3 | 8.1 | | | | | | | |
| | | Prag_222 | 827 | 55.1 | 6.4 | 7.7 | | | | | | | |
| | | Prag_232 | 5343 | 47.4 | 6.5 | 7.2 | | | | | | | |
| | | Prag_242 | 1014 | 59.0 | 6.2 | 10.0 | | | | | | | |
| | | Prag_252 | 5876 | 49.4 | 6.4 | 8.2 | | | | | | | |
| | | Prag_262 | 1091 | 97.6 | 8.4 | 11.3 | | | | | | | |
| | | Prag_272 | 546 | 40.5 | 6.7 | 6.4 | | | | | | | |
| | | Prag_282 | 854 | 70.4 | 7.0 | 9.1 | | | | | | | |
| Mean values | | | 1436.2 | 54.7 | 6.0 | 8.6 | | | | | | | |

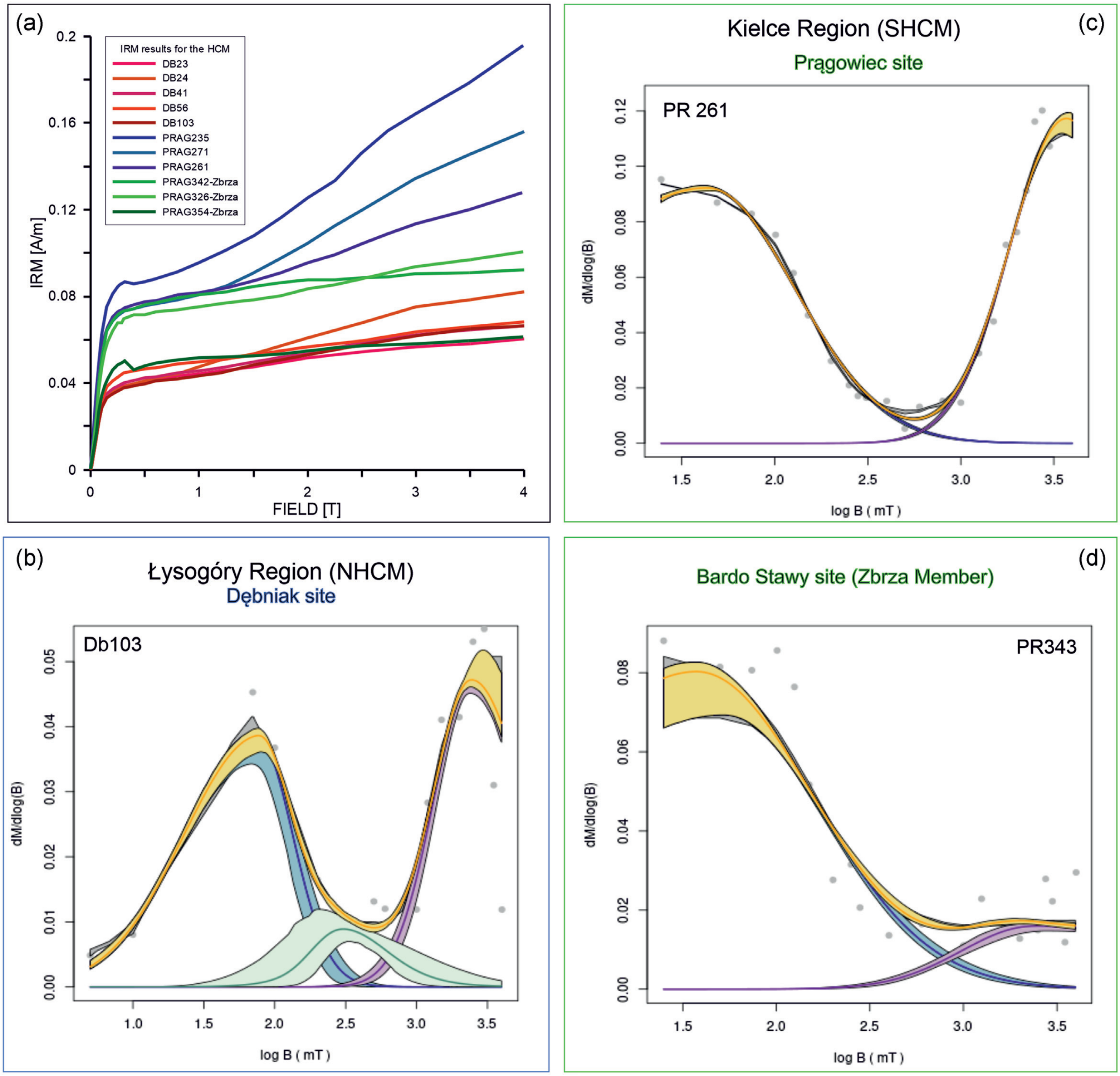


**Figure 5.** (a) IRM acquisition for selected samples from the HCM area from three sites including the Dębniak Beds (DB), the Prągowiec Beds (PRAG), and the Zbrza Member (PRAG-Zbrza). Model fit examples for the specimens from the Dębniak Beds (b) with 3 components model, from the Prągowiec Beds (c), and from the Bardo Stawy site from the Zbrza Member (d) with 2 components models. Coercivity distribution is derived from IRM demagnetization (grey circles - data, a spline fit partially visible as black line) measurements. Abbreviations: yellow - model, blue – component 1, purple – component 2, green – component 3. The shaded area represents error envelopes of 95 per cent confidence intervals; in the cases where no shading is present, confidence intervals are thinner than the line (after Maxbauer *et al*., 2016).

causes continuous loss of remanence over wide ranges of temperature, which may obscure the evidence of the transition (e.g. Liu *et al*. 2006). Significant recovery of the RT-SIRM on rewarming and higher intensity of FC than ZFC SIRM suggest the occurrence of a single domain (SD) magnetite, and no MD magnetite identified (e.g. Moskowitz *et al*. 1993; Carter-Stiglitz *et al*. 2006; Jackson *et al*. 2011). Further, the results of IRM decomposition for the low coercivity component have a wide range of *DP* and vary from 0.4 to 0.67. A higher *DP* value (>0.5) may be an indicator of mixed mineralogy and mixed grain size within a single component (Heslop *et al*. 2004; Maxbauer *et al*. 2016). Considering the thermal evolution of both parts of the HCM, where maximal burial temperatures are generally above 100 °C (e.g. Narkiewicz *et al*. 2010; Marynowski 1999; Smolarek *et al*. 2014; Schito *et al*. 2017; Środoń & Trela 2012), the diagenetic origin of small (SD) magnetite grains is the most likely. Interestingly, the recent studies by Hounslow *et al*. (2021) based on relationships in geochemistry, found the detrital origin of magnetite (also hematite and Fe-bearing silicates) in Telychian (Silurian) grey-mudstones from the Polish margin of the East European Craton (EEC). It is worth noting, however, that the site locations investigated in this research belong to the Podlasie and Bug Depressions Silurian sub-basins and they are relatively closer

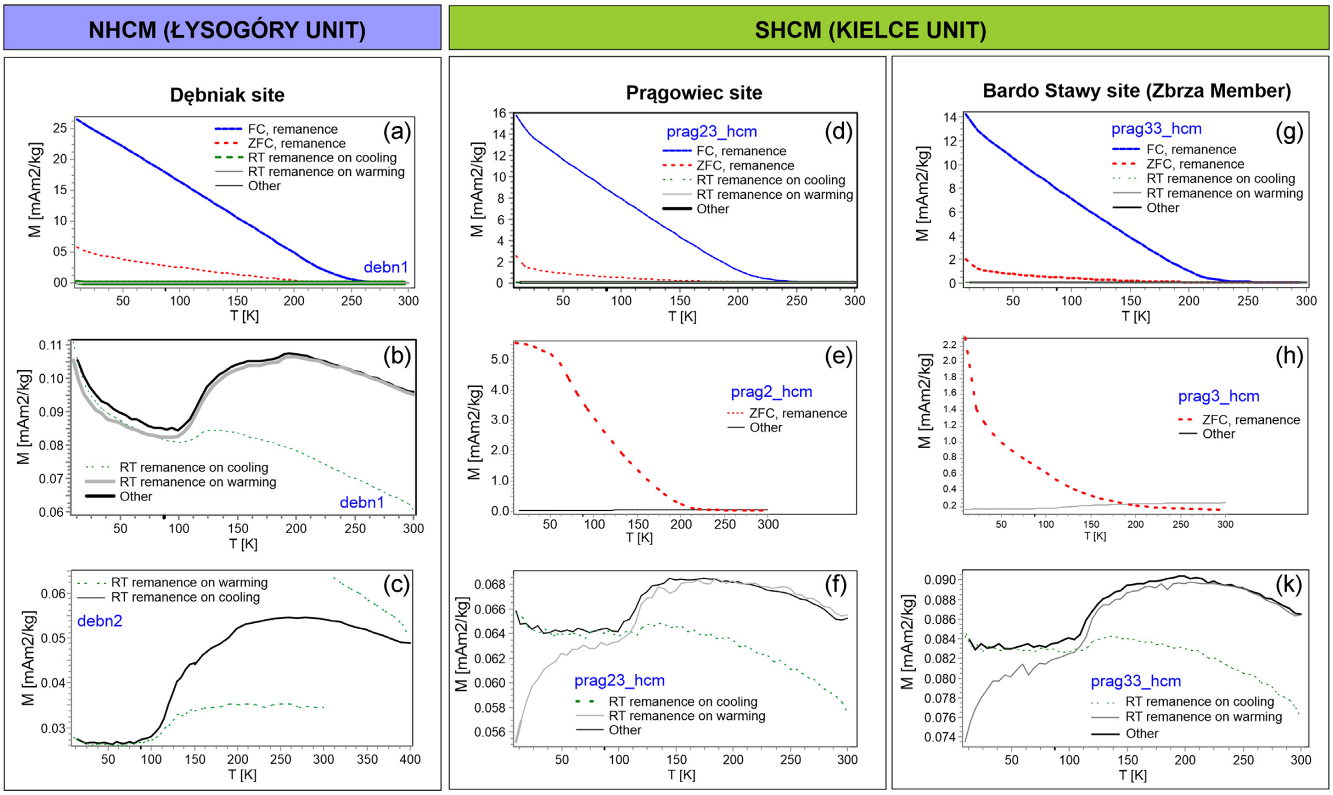


**Figure 6.** Results of low temperature (300–10 K range; –263.15 to 26.85 °C) remanence measurements for selected specimens of (a, b and c) the Dębniak Beds (NHCM), (d, e, f) the Prągowiec Formation, and (g, h, k) black shales of the Zbrza Member from the Bardo Stawy site (SHCM). Abbreviations: Zero Field Cooled (ZFC), Field Cooled (FC), Room Temperature Saturated Isothermal Remanent Magnetization (RT-SIRM), the 'Other' curves are the results of the RT-SIRM performed while cooling in a small (+5 µT) applied magnetic field. Note, the three upper charts (a, d and g) present the whole sequence applied on the selected specimen (see Section 3.2. for more details), while the bottom (c, f and k) show the same curves, but RT-SIRM only. Here, on the chart (c) note a hump on RT- remanence on warming and 'Other' curve around 200 K, attributed to the presence of hematite grains. The three charts in the middle represent (b) sequence aiming to confirm the presence of goethite with visible Néel temperature ($T_N$), whereas (e and h) show the difference between the ZFC remanence curve (see the details in Section 4.2).

to the land area than both the HCM parts (see Teller, 1997). Also, the depth of these sedimentary sub-basins was relatively lower than for the HCM area, defined as a deep-water zone (op. cit.). We found no traces of detrital magnetite grains in the studied Silurian shales of HCM, and in our opinion, they are missing or very little, as they were likely dissolved during diagenesis. Likewise, the burial evolution of the HCM excludes the occurrence of magnetofossils potentially abundant in ancient marine sediments as dissolved (after Schwartz *et al*. 1997; Kopp & Kirschvink 2008).

The presence of such widespread minerals as goethite is generally attributed to the weathering of iron-bearing minerals after exhumation, or to processes like oxidation of $Fe^{2+}$dissolved in the sediment column, but it can occur also as a detrital phase in marine sediments (e.g. Heller 1978; Van der Zee *et al*. 2003; Till *et al*. 2015). The studied Silurian rocks were exposed to weathering a few times, the most recently during Neogene time, and earlier during the Late Cretaceous, when the HCM area underwent inversion (Kutek & Głazek 1972; Dadlez & Marek 1997; Dadlez *et al*. 1998; Hakenberg & Świdrowska 1998; Krzywiec 2007; Świdrowska & Hakenberg 2008; Krzywiec *et al*. 2009). As the collected samples were excavated from an outcrop, thus, goethite is supposed to form during weathering, and in our opinion, the most likely is a strong impact of the latest one (Neogene).

Considering the early diagenetic origin model for goethite presented by Kiipli *et al*. (2000) for Baltica it is worth discussing it in the context of the NHCM area, even though we suggest the weathering origin is plausible. Their observations of Telychian marine red beds of the East Baltic suggest that goethite (and hematite) in the oxic marine environment with pH near 8 favor its formation from ferrihydrite. However, the recent work of Van der Zee *et al*. (2003) demonstrated that direct goethite precipitation, in the lake and marine sediments, occurs near the oxic-anoxic boundaries. Therefore, in the generally suboxic marine environment of the NHCM sub-basin with only temporary oxygen enrichment episodes (see Trela *et al*. 2016), autogenic goethite might have been formed. However, the argument against autogenous origin is the $T_N$, which ranges between 120 and 130 °C (Fig. 6b, see Section 4.2 for details), characteristic of well-crystallized goethite (e.g. Dekkers 1989b; Ozdemir & Dunlop 1996), whereas in Van der Zee *et al*. (2003)'s research, nanocrystals contaminated during precipitation were suggested as a product of goethite autogenic formation.

### 5.1.2 *Hematite and maghemite*

In contrast to the Prągowiec and Bardo Stawy beds (SHCM), the results of thermal demagnetization of three-component IRM (see Fig. 4c), IRM decomposition (Fig. 5b), and low-temperature SIRM (Figs 6b and c) confirm the presence of hematite and/or maghemite in the Dębniak Beds. The Morin transition observed

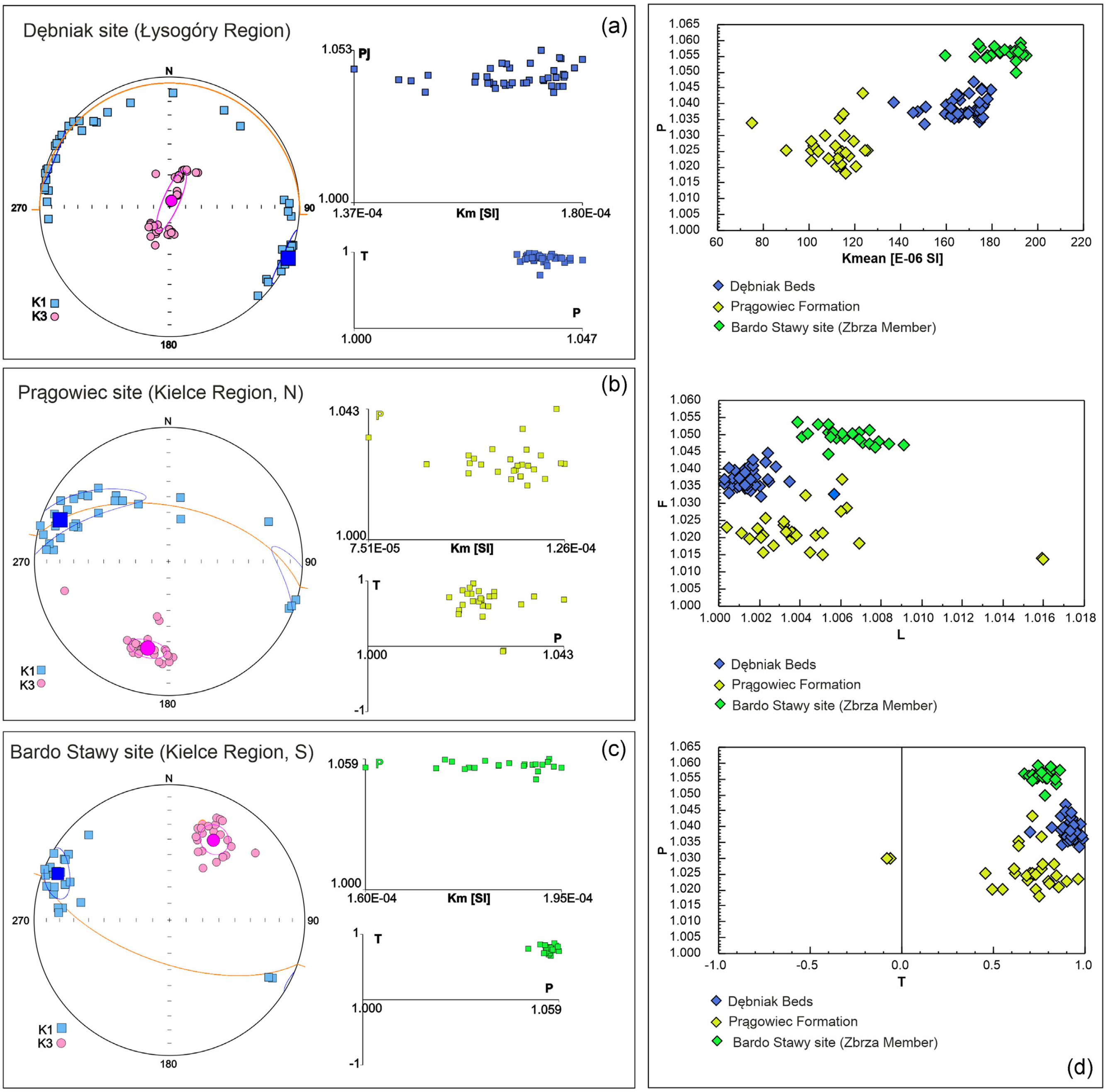


**Figure 7.** Results of anisotropy of magnetic susceptibility of specimens from the (a) Dębniak Beds (the NHCM), (b) Prągowiec and (c) Zbrza Member beds from the Bardo Stawy site (the SHCM), (d) parameters comparison for all sites together. Abbreviations: K1 – maximal AMS axis, K3 – minimal AMS axis, intensive color represents mean directions, orange line – bedding plane, Km – mean susceptibility, T – shape parameter of the ellipsoid, P – degree of AMS, F – magnetic foliation, L – magnetic lineation.

at approximately 190 K (−83.15 °C) may suggest hematite grain size nanoparticles of about 40–90 nm in diameter (Özdemir *et al.* 2008), which corresponds with SD-like behavior (Kletetschka & Wasilewski 2002). The small size of nanoparticles, determining recovered remanence, can explain only slightly visible Morin transition (Chevallier & Mathieu 1943; Bando *et al.* 1965), and lower temperatures (approximately 190 K, Figs 6b and c) of the observed transition (Özdemir *et al.* 2008). Similar conclusions come from the IRM decomposition, where $B_h$ of 2.56 (±0.06) log10 units (366 mT) and *DP* of 0.27 (±0.06) suggest fine-grained hematite, oxidized magnetite or maghemite.

*5.1.2.1 Plausible detrital origin* In the context of inconsistent hematite distribution in examined sites, an important question is what kind of factors determined the hematite formation. Generally, high coercivity minerals, like hematite, are more resistant to dissolution in marine waters than for example magnetite (Abrajevitch *et al.* 2009), and their grains were found even in anoxic environments at greater depths than magnetite (e.g. Yamazaki *et al.* 2003; Emiroglu *et al.* 2004; Liu *et al.* 2004; Garming *et al.* 2005), even in organic-rich layers (Robinson *et al.* 2000). Recently provided models explaining hematite presence in marine sediments propose a direct detrital transport of this mineral, involving aeolian processes, hyperpycnal flood events, or turbidity currents (e.g. Kruiver *et al*. 2000; Balsam *et al*. 2007; Channell *et al*. 2013). Here, the relatively close distance between the NHCM sedimentary sub-basin and the Baltica continent (see Nawrocki *et al*. 2007; Torsvik *et al*. 2017) allows us to interpret that hematite was likely continentally delivered through aeolian transport (no turbidity currents were observed in the studied rocks). The most recent research published by Hounslow *et al*. (2021) is in line with this scenario, showing evidence of the Telychian oxygenation event on the Polish margin of the EEC. The authors suggest the event is associated with a reduction in primary palaeoproductivity resulting from greater aridity on the EEC, which can be linked to decreased nutrient input to the Polish margin, with simultaneously enhanced aeolian inputs from Fe-enriched soils (see Hounslow *et al*. 2021 for further details). A similar outcome can be found, for instance, in studies by Clemens & Prell (1991), who proposed ferrimagnetic grains being supplied during Quarternary glacial stages in the Arabian Sea sediments due to an increased supply of aeolian dust during glacial periods resulting from increased aridity and/or wind speed. These arguments show (1) hematite grains as resistant in the marine environment, (2) the NHCM with a relatively close distance to the source of detritus from the arid EEC iron-rich soils and (3) enhanced aeolian activity during glacial stages in Telychian times. Bearing them together, in our opinion, the most likely scenario is continentally delivered detrital hematite.

*5.1.2.2 Early and late diagenetic origins consideration* Even if in our opinion the presented framework of hematite origin is the most likely, it is worth discussing (1) the early diagenetic origin from previously proposed scenarios (Kiipli *et al*. 2000; Trela *et al*. 2016), and the late diagenetic origin, (2) burial and (3) weathering, as generally elevated temperatures were observed in the HCM rocks as well as episodes of meteoric fluids penetration.

(1) The model of the authigenic origin of hematite and goethite put forward by Kiipli *et al*. (2000), suggests re-oxygenation of shelf bottom waters in the East Baltica as a main controlling factor, which can be considered by the fact of temporary benthic oxygen increase demonstrated also in the Dębniak Beds mudstones (Trela *et al*. 2016). Thus, the formation of hematite through ferrihydrite reaction under oxidative conditions should be debated here. The results of Van der Zee *et al*. (2003), showed however, that the main diagenetic reactive precipitate in aquatic sediments under oxidative conditions leads to the formation of goethite, instead of hematite as suggested earlier by, for example Schwertmann & Murad (1983). Therefore, we consider the hypothesis of autogenic hematite in the NHCM area as doubtful.

(2) Briefly considering hematite formation associated with burial diagenetic alterations (see Channell *et al*. 1982; Till *et al*. 2015, as well as Dekkers 1988, 1989b; Özdemir & Dunlop 1996; Ruan *et al*. 2001; Przepiera & Przepiera 2003; Cudennec & Lecerf 2005; for the process details), we can reject dihydroxylation of goethite or other oxy-hydroxides as the factor determining hematite formation in the NHCM area solely. Even if the subsidence and thickness of sediments of the NHCM area were higher than in the SHCM, and thus the temperature range which analyzed rocks experienced (<200 °C), the burial conditions were not sufficient enough for the transformation of goethite into hematite. Also, the same argument allows rejecting hematite as a product of maghemite alteration in elevated (above 250 °C) temperatures (e.g. Bernal *et al*. 1957; Özdemir & Banerjee 1984; Özdemir & Dunlop 1988; Özdemir 1990).

(3) The late diagenetic origin of magnetic mineral (including hematite), caused by the downward migration of oxidizing meteoric fluids during Permian–Triassic palaeoweathering in the HCM, discussed earlier by, for example Szulczewski (1995), Grabowski *et al*. (2006), Szaniawski (2008) and Marynowski *et al*. (2017) can be efficiently rejected for NHCM mudstones. The examined Dębniak Formation (NHCM) during the Permian-Triassic was covered by Silurian and Devonian rocks of a significant thickness (Fig. 2). Therefore, the Dębniak Beds could not be easily penetrated by oxidizing fluids as Carboniferous shales (25 m thick, after Szulczewski *et al*. 1996) or reddish Devonian carbonates, in which karstification marks are visible (Marynowski *et al*. 2017). Therefore, we consider the late diagenetic origin of hematite unlikely.

### 5.2 Magnetic mineral assemblage and its provenance interpretation

Timing of the NHCM (the Łysogóry terrane) docking, and generally its paleoposition during early Paleozoic times concerning the SHCM (the Małopolska Block) and Baltica is still controversial and various scenarios were proposed (e.g. Winchester 2002; Nawrocki *et al*. 2007). Origin as an exotic terrane that was derived from the Gondwana margin and brought closer to Baltica during the Late Cambrian was proposed by Bełka *et al*. (2002). Winchester & PACE TMR Network Team (2002) questioned the origin of these terranes as a part of Eastern Avalonia and postulated that both NHCM and SHCM had moved to the vicinity of the Baltica earlier than this microcontinent. They also suggested that the timing of the docking of the NHCM terrane with Baltica appears to be later than the SHCM. On the other hand, the seismic analyzes of Malinowski *et al*. (2005) and interdisciplinary studies of Nawrocki *et al*. (2007) pointed to a stationary model for the NHCM and its close link with the mobile edge of the EEC, which supported the previous observations of, for example Dadlez (1995). At the same time, the detritus examined from the Upper Silurian grey-wackes for both parts of the HCM studies indicate a continental island arc provenance of the material (Kozłowski *et al*. 2004).

Our findings, therefore, are in line with previously proposed scenarios postulated by researchers like Dadlez (1995) or later by Nawrocki *et al*. (2007), and observations based on the sedimentary and seismic studies (see Malinowski *et al*. 2005 for more details). In our opinion, the relatively close distance between the NHCM and Baltica allowed for detrital transportation from the continent, and then the deposition of magnetic mineral, hematite, in the early Silurian marine environment. During this time the global eustatic events were sufficient enough to mask most of the effects related to the local tectonism in the HCM area, and thus Telychian grey mudstones in the NHCM were deposited in a generally suboxic environment with only seasonal ventilation episodes (Trela *et al*. 2016; Smolarek *et al*. 2017; Trela 2021). In our opinion, the local tectonism of the HCM area or temporal oxygenation of the water column had only a minor, if any, influence on the precipitation or modification of hematite, as high-coercivity minerals (e.g. hematite) are generally resistant to reductive dissolution (e.g. Robinson *et al*. 2000; Yamazaki *et al*. 2003, Emiroglu *et al*. 2004, Liu *et al*. 2004, Garming *et al*. 2005; Abrajevitch *et al*. 2009). Therefore, the most important aspect of hematite presence in examined marine sediments of the Dębniak Beds is the relatively close distance to the sediment supply area, which can be considered as a main determinant of hematite grains preserved solely in the NHCM. The studies of Hounslow *et al*. (2021) are consistent with this scenario, providing evidence of an enhanced detrital hematite content in Silurian (Telychian) marine sediments from northern Europe (similar to the studied Dębniak Beds), resulting from increased aridity and aeolian transportation of ferroan-rich detrital material from Baltica continent. This record can also be detected in the Polish margin of the EEC (see Hounslow *et al*. 2021 for more details). Summarizing, we suggest that the position of the NHCM in early Silurian times was relatively closer to Baltica than the SHCM, as high coercivity and resistant to dissolution hematite grains of detrital (aeolian) origin, were preserved solely in the NHCM Silurian (Telychian) marine sediments.

### 5.3 Magnetic anisotropy and its palaeotectonic interpretation

The results of petromagnetic analyses (susceptibility versus temperature curves and hysteresis loops) imply that magnetic susceptibility is mainly controlled by paramagnetic minerals, presumably in the main by phyllosilicates being the main rock-forming mineral in studied shales (Masiak *et al*. 2003; Mustafa *et al*. 2015). Thereby preferred orientation of these minerals determines magnetic fabrics expressed by the AMS results. Oblate AMS ellipsoid and distinct bedding parallel foliation document dominant sedimentary-compactional alignment of phyllosilicate plates, which is typical for weakly deformed dark shales (e.g. Chadima *et al*. 2004; Wenk *et al*. 2010; Niezabitowska *et al*. 2019a).

All sampled sites reveal feeble magnetic lineation characterized by WNW–ESE grouping of maximal AMS axes regardless of generally oblate AMS ellipsoids (Fig. 7). Similar magnetic fabrics in all sites suggest a consistent genesis of this lineation for both parts of the HCM. WNW–ESE lineation is parallel to the strike line measured in the field and to the general regional structural trend expressed by the orientation of the HCF and axes of regional kilometer-scale fold structures (Czarnocki 1957; Bugajska-Pająk *et al*. 1961; Lamarche 1999, 2002). Furthermore, two sites were sampled from steep limbs of the Bardo Syncline (the Prągowiec and Zbrza sites). These observations imply the tectonic origin of the lineation. However, only a small modification of dominantly planar, sedimentary magnetic fabric indicates that the tectonic strain, which affected studied rocks and led to the formation of the lineation, was relatively weak. This corresponds to our field observations indicating the lack of cleavage in all studied rocks.

An exhaustive explanation of the magnetic lineation genesis is more puzzling, especially its relation to the particular deformation episodes/phases. The first and most probable interpretation is its Variscan origin as it is parallel to the axis of the main Variscan map-scale folds and perpendicular to the Variscan strain determined from structural studies (Czarnocki 1957; Lamarche *et al*. 1999, 2003b). However, this model is not the only one that can explain the results. Where the Maastrichtian-Paleocene deformation episode can be likely rejected as the main factor determining observed lineation, the Caledonian origin of the lineation cannot be excluded. The Maastrichtian-Palaeocene deformations had a rather weak and mostly brittle character within the internal parts of the Palaeozoic basement (more intense deformations were reported mainly from the contact zone of Palaeozoic substratum and its Mesozoic cover, see e.g. Lamarche 1999, 2003b; Konon & Mastella 2001; Szaniawski *et al*. 2011, for more details). In turn, among many different interpretations explaining the scale and mechanism of the Caledonian deformation in the HCM (e.g. Znosko, 1986, 2000; Dadlez *et al*. 1994; Mizerski 1995), some models assume Caledonian thrusting or reverse faulting along the HCF (Gągała 2015). The later deformation mechanism is matching with the WNW–ESE lineation documented in these studies. The local importance of Caledonian deformations in the study area suggests also cartographic outcomes from the Bardo Syncline implying unconformity between lower and upper Palaeozoic strata (e.g. Bugajska-Pająk *et al*. 1961; Znosko 1986). In conclusion, it is possible that the observed lineation is partially Caledonian in origin and further reinforced or entirely overprinted by Variscan shortening with similar stress field geometry.

Regardless of the lineation age, the horizontal orientation of AMS maximal axes fits better with deformation models assuming thrusting or reverse faulting activity of the HCF (e.g. Stupnicka 1988; Gągała 2015) rather than its regional-scale strike-slip kinematics (e.g. Nawrocki *et al*. 2007; Kozłowski 2008; Lamarche *et al*. 2003a; Konon 2007). This, however, requires confirmation by specialized studies based on a larger magnetic fabric data set obtained from rocks of different ages and tectonic positions, which differs from the thematic scope of these studies.

## 6 CONCLUSIONS

(i) In all analysed samples of Silurian graptolite shales nearly stoichiometric SD magnetite was identified. The origin of this mineral is likely diagenetic as the rocks from both parts of the HCM, the NHCM and SHCM, were buried over 100 °C. No traces of detrital magnetite were found, what we associate with diagenetic dissolution. In turn, goethite has most likely a recent Neogene-time weathering origin.

(ii) In contrast to the SHCM, in the northern part of the HCM, in the sampled Dębniak Beds presence of SD hematite and/or maghemite was determined. We attribute their appearance to detrital transport, specifically to the aeolian processes. In our opinion, the NHCM has had a more proximal location than the SHCM concerning the Baltica continent during early Silurian times, hence the presence of hematite transported from the nearby onshore EEC, which was dry and nutrient-poor.

(iii) Even if it is accepted that during late Llandovery (Silurian), generally, a more aerobic environment characterizes bottom water conditions in the present NHCM than in the SHCM, we rather reject reactions in oxygenic waters of hemipelagic environments as a potential source of hematite and/or maghemite.

(iv) The presented AMS data allowed us to conclude that the observed magnetic fabric has a dominantly sedimentary origin with only a weak record of tectonic strain related most probably to Variscian deformations.

Further studies should consider the environmental changes monitoring through the profile starting from early Ordovician to early Devonian times. Also, more sample sites from both parts of the HCM will better understand the Silurian palaeogeography of this part of Europe and allow a more comprehensive recognition of the relationships between magnetic mineral composition and the marine environment.

## ACKNOWLEDGMENTS

DKN was supported by the National Science Centre, Poland (No. UMO-2019/32/T/ST10/00479), within the Etiuda 7 scholarship. This research has been funded by The National Centre for Research and Development (NCBR) within the Blue Gas project (No

BG2/SHALEMECH/14). Part of this work was performed as a Visiting Scholar at the Institute for Rock Magnetism (IRM) at the University of Minnesota. The IRM is a US National Multi-user Facility supported through The U.S. National Science Foundation, Earth Sciences Division, and by funding from the University of Minnesota.

## DATA AVAILABILITY STATEMENT

The data underlying this paper are available in the paper.

## CONFLICT OF INTEREST

Authors declare no conflict of interest.

## AUTHOR CONTRIBUTIONS

Conceptualization: DN and RS; Data curation: DN; Methodology: DN and RS; Formal analysis: DN and RS; Funding acquisition: DN and RS; Investigation: DN; Visualization: DN; Writing—original draft preparation: DN; Writing—review and editing: DN and RS. Both authors have read and agreed to the published version of the paper.

## REFERENCES

Abrajevitch, A., Van Der Voo, R. & Rea, D.K. 2009.Variations in relative abundances of goethite and hematite in Bengal Fan sediments: climatic vs. diagenetic signals, *Mar. Geol.,* **267**(3–4), 191–206.

Aragón, R., Buttrey, D.J., Shepherd, J.P. & Honig, J.M. 1985. Influence of nonstoichiometry on the Verwey transition, *Phys. Rev. B.,* **31,** 430–436.

Aubourg, C. & Pozzi, J.-P. 2010. Toward a new <250° C pyrrhotite-magnetite geothermometer for claystones, *Earth planet. Sci. Lett.,* **294**(1-2), 47–57.

Balsam, W., Arimoto, R., JI, J., Shen, Z. & Chen, J. 2007. Aeolian dust in sediment: a re-examination of methods for identification and dispersal assessed by diffuse reflectance spectrophotometry, *Int. J. Environ. Health,* **1**(3), 374–402.

Bando, Y., Kiyama, M., Yamamoto, N., Takada, T., Shinjo, T. & Takaki, H. 1965. The magnetic properties of $\alpha$-$Fe_2O_3$, *J. Phys. Soc. Jpn.,* **20,** doi:10.1143/JPSJ.20.2086.

Banerjee, S.K., Hunt, C.P. & Liu, X.-M. 1993. Separation of local signals from the regional paleomonsoon record of the Chinese loess plateau: a rock-magnetic approach, *Geophys. Res. Lett.,* **20,** 843–846.

Barker, C. E. & Pawlewicz, M. J. 1994. Calculation of vitrinite reflectance from thermal histories and peak temperatures. A comparison of methods, in *Vitrinite Reflectance as a Maturity Parameter, Applications and Limitations,* pp. 216–229, American Chemical Society Symposium Series 570, eds Mukhopadhyay, P. K. & Dow, W. G., American Chemical Society.

Bednarczyk, W. S., Chlebowski , R. & Kowalczewski, Z. 1970. Budowa geologiczna północnego skrzydła Antykliny Dymińskiej w Górach Świętokrzyskich, *Biuletyn Geologiczny,* **12,** 197–223.

Bełka, Z. 1990. Thermal maturation and burial history from conodoncolor alteration data, Holy Cross Mountains, Poland, *Courier Forschungs institut Senckenberg,***118,** 241–251.

Belka, Z., Ahrendt, H., Franke, W. & Wemmer, K. 2000. The Baltica-Gondwana suture in central Europe: evidence from K-Ar ages of detrital muscovites and biogeographical data, *Geol. Soc. Lond. Spec. Publ.,* **179,** 87–102.

Bełka, Z., Valverde-Vaquero, P., Dörr, W., Ahrendt, H., Wemmer, K., Franke, W. & Schäfer, J. 2002. Accretion of first Gondwana-derived terranes at the margin of Baltica, *Geol. Soc. Lond. Spec. Publ.,* **201,** 19–36.

Bernal, J.D., Dasgupta, D.R & Mackay, A.L. 1957. Oriented transformation in iron oxides and hydroxides, *Nature,* **180,**645–647.

Bond, D.P.G. & Grasby, S.E. 2017. On the causes of mass extinctions, *Palaeogeogr., Palaeoclimatol., Palaeoecol.,* **478,** 3–29.

Botor, D., Anczkiewicz, A. A., Dunkl, I., Golonka, J., Paszkowski , M. & Mazur, S. 2018. Tectonothermal history of the Holy Cross Mountains (Poland) in the light of low-temperature thermochronology, *Terra Nova,* **30,** 270–278.

Bugajska-Pająk A., *et al.* 1961. Mapa geologiczna regionu świętokrzyskiego bez utworów czwartorzędowych. 1: 200 000. Warszawa: Wydaw. Geol. 1961 sygn. K-81.

Carter-Stiglitz, B., Moskowitz, B. & Jackson, M. 2004. More on the low-temperature magnetism of stable single domain magnetite: reversibility and non-stoichiometry, *Geophys. Res. Lett.,***31**(6), doi:10.1029/2003GL019155.

Carter-Stiglitz, B.S., Moskowitz, B., Solheid, P., Berquó, T.S., Jackson, M. & Kosterov, A. 2006. Low-temperature magnetic behavior of multi-domain titanomagnetites: TM0, TM16, and TM35, *J. geophys. Res.,***111**(B12), doi:10.1029/2006JB004561.

Chadima, M., Hansen, A., Hit, A.M., Hrouda, F. & Siemes, H. 2004. *Phyllosilicate preferred orientation as control of magnetic fabric: evidence from neutron texture goniometry and low and high-field magnetic anisotropy (SE Rhenohercynian Zone of Bohemian Massif),* Geol. Soc., Lond., Spec. Publ., **238,** 361–380.

Channell, J., Freeman, R., Heller, F. & Lowrie, W. 1982. Timing of diagenetic haematite growth in red pelagic limestones from Gubbio (Italy), *Earth planet. Sci. Lett.,* **58,** 189–201.

Channell, J.E.T., Hodell, D.A., Margari, V., Skinner, L.C., Tzedakis, P.C. & Kesler, M.S. 2013. Biogenic magnetite, detrital hematite, and relative paleointensity in Quaternary sediments from the Southwest Iberian Margin, *Earth planet. Sci. Lett.,* **376,** 99–109.

Chevallier, R. & Mathieu, S. 1943. Proprietes magnetiques des poudres d'hematite-influence des dimensions des grains, *Ann. Phys.,* **11**(18), 258–288.

Clemens , S.C. & Prell, W.L. 1991. One million-year record of summer monsoon winds and continental aridity from the Owen Ridge (Site 722), northwest Arabian Sea, *Proc. Ocean Drill. Prog. Sci. Results,* **117,** 365–388.

Cocks, L.R.M. 2002. Key Lower Palaeozoic faunas from near the Trans European Suture Zone, *Geol. Soc., Lond., Spec. Publ.,* **201,** 3–46.

Cocks , R.M. & Torsvik, T.H. 2005. Baltica from the late Precambrian to mid-Palaeozoic times: the gain and loss of a terrane's identity, *Earth-Sci. Rev.,* **72**(1–2), 39–66.

Crampton, J.S., Cooper, R.A., Sadler, P.M. & Foote, M. 2016. Greenhouse−icehouse transition in the Late Ordovician marks a step-change in the extinction regime in marine plankton, *Proc. Natl. Acad Sci,* **113,** 1498–1503.

Cudennec, Y. & Lecerf, A. 2005. Topotactic transformations of goethite and lepidocrocite into hematite and maghemite, *Solid State Sci.,* **7,** 520–529.

Czarnocki, J. 1950. Geologia regionu łysogórskiego w związku z zagadnieniem złoża rud żelaza w Rudkach. *Pr. Inst. Geol.,* 40.

Czarnocki, J. 1957. Prace geologiczne. T. 2. Tektonika Gór Świętokrzyskich, Z. 1. Stratygrafia i tektonika Gór Świętokrzyskich. Pr. Inst. Geol. 18. t. 2, z. 1.

Dadlez, R. 1995. Debates about pre-Variscan tectonics of Poland, *Stud. Geophys. Geod.,* **39,** 227–234,

DadleZ, R., KowalczewskI, Z. & Znosko, J. 1994. Some key problems of the pre-Permian tectonics of Poland, *Geol. Quart.,* **38**(2), 169–190.

Dadlez, R. & Marek , S. 1997. Rozwój basenów permu i mezozoiku, in *The epicontinental Permian and Mesozoic in Poland,* Vol. **153,** pp. 403–409, eds Marek, S. & Pajchlowa, M., Prace Państwowego Instytutu Geologicznego.

Dadlez, R., Marek, S. & Pokorski , J. 1998. *Paleogeographic atlas of epicontinental Permian and Mesozoic in Poland (1:2 500 000),* Warszawa, Polish Geological Institute, 7 pp, 75 plates - maps and cross-sections.

Davies, J. R., Waters, R.A., Molyneux, S. G., Williams, M., Zalasiewicz, J.A. & Vandenbroucke, Thijs R.A. 2016. Gauging the impact of glacioeustasy on a mid-latitude early Silurian basin margin, mid-Wales, UK, *Earth-Sci. Rev.,* **156,** 82–107.

Deczkowski, Z. & Tomczyk, H. 1969. Starszy paleozoik z otworu Wilków (północna część Gór Świętokrzyskich), *Geol. Quart.,* **13,** 14–26.

Dekkers, M.J. 1988. Magnetic Behavior of Natural Goethite During Thermal Demagnetization, *Geophys. Res. Lett.,* **15,** 538–541.

Dekkers, M.J. 1989a. Magnetic properties of natural pyrrhotite. II. High- and low-temperature behavior of $J_{RS}$ and TRM as a function of grain size, *Phys. Earth planet. Inter.,* **57**(3–4), 266–283.

Dekkers, M.J. 1989b. Magnetic properties of natural goethite – II. TRM behavior during thermal and alternating field demagnetization and low-temperature treatment, *Geophys. J. Int.,* **97,** 341–355.

Dekkers, M.J., Mattei, J.-L., Fillion, G. & Rochette, P. 1989. Grain-size dependence of the magnetic behavior of pyrrhotite during its low-temperature transition at 34 K, *Geophys. Res. Lett.,* **16**(8), 855–858.

Emiroglu, S., Rey, D. & Petersen, N. 2004. Magnetic properties of sediment in the Ria de Arousa (Spain): dissolution of iron oxides and formation of iron sulfides, *Phys. Chem. Earth,* **29,** 947–959.

Fillion, G. & Rochette, P. 1988. The low-temperature transition in monoclinic pyrrhotite, *J. Phys. Colloq.,* **49**(C8), C8–907-C8-908.

Filonowicz, P. 1971. Geological map of Poland, Kielce sheet, scale 1:50 000. Wydawnictwa Geologiczne; Warszawa.

Gągała, Ł. 2015. Late Silurian deformation in the Łysogóry Region of the Holy Cross Mountains revisited: restoration of a progressive Caledonian unconformity in the Klonów Anticline and its implications for the kinematics of the Holy Cross Fault (central Poland), *Geol. Quart.,* **59**(3), doi:10.7306/gq.1222.

Garming, J.F.L. & Bleil, U., 2005. Alteration of magnetic mineralogy at the sulfate–methane transition: analysis of sediments from the Argentine continental slope, *Phys. Earth planet. Inter.,* **151,** 290–308.

Głazek, J., Karwowski, L., Racki , G. & Wrzołek, T. 1981. The early Devonian continental/marine succession at Chęciny in the Holy Cross Mountains, and its paleogeographic and tectonic significance, *Acta Geol. Polonica,* **34,** 233–254.

Grabowski, J., Narkiewicz, M. & Sobień, K. 2006. Thermal controls on the remagnetization of Devonian carbonate rocks in the Kielce region (Holy Cross Mts.) (in Polish with English summary), *Przegląd Geologiczny,* **54**(10), 895–905.

Guterch, A., Materzok, R., Pajchel, J., Perchuc, E., Grad, M. & Toporkiewicz, S. 1984. Deep structure of the earth's crust in the contact zone of the Paleozoic and Precambrian Platforms and the Carpathian Mts in Poland, *Acta Geophys. Polonica,* **32**(1), 25–41.

Hakenberg, M. & Świdrowska, J. 1998. Evolution of the Holy Cross segment of the Mid-Polish Trough during the Cretaceous, *Geol. Quart.,* **42,** 239–262.

Halgedahl, S. & Jarrard, R.D. 1995. Low-temperature behavior of single domain through multidomain magnetite, *Earth planet. Sci. Lett.,* **130,** 127–139.

Heller, F. 1978. Rock magnetic studies of Upper Jurassic limestones from southern Germany, *J. Geophys.,* **44,** 525–543.

Heslop, D., Mcintosh, G. & Dekkers, M.J. 2004. Using time and temperature-dependent Preisach models to investigate the limitations of modeling isothermal remanent magnetization acquisition curves with cumulative log Gaussian functions, *Geophys. J. Int.,* **157,**55–63.

Hounslow , M.W., Ratcliffe, K. T., Harris, S.E., Nawrocki, J., Wójcik, K., Montgomery, P. & Woodcock, N.H. 2021. The Telychian (early Silurian) oxygenation event in northern Europe: a geochemical and magnetic perspective, *Palaeogeogr., Palaeoclimatol., Palaeoecol.,* **567,** doi:10.1016/j.palaeo.2021.110277.

Hrouda, F. 1982. Magnetic anisotropy of rocks and its application in geology and geophysics, *Geophys. Surv.,* **5**(1), 37–82.

Hrouda, F. 1994. A technique for the measurement of thermal changes of magnetic susceptibility of weakly magnetic rocks by the CS-2 apparatus and KLY-2 Kappabridge, *Geophys. J. Int.,* **118**(3), 604–612.

Hrouda, F., Jelinek, V. & Zapletal, K. 1997. Refined technique for susceptibility resolution into ferromagnetic and paramagnetic components bases on susceptibility temperature variations measurement, *Geophys. J. Int.,* **129**(3), 715–719.

Hunt, C.P., Banerjee, S.K., Han, J., Solheid, P.A., Oches, E., Sun, W. & Liu, T. 1995. Rock-magnetic proxies of climate change in the loess-paleosol sequences of the western Loess Plateau of China, *Geophys. J. Int.,* **123,** 232–244.

Jackson, M., Bowles, J., B& anerjee, S. 2011. Interpretation of low-temperature data. Part V: the magnetite Verwey transition (Part B): field-cooling effects on stoichiometric magnetite below TV, *IRM Quart.,* **21**(4), 1–11.

Jaworowski, K. 1971. Sedimentary structures of the Upper Silurian siltstones in the Polish Lowlands, *Acta Geol. Polonica,* **21,** 519–571.

Jaworowski, K. 2000. Facies analysis of the Silurian shale-siltstone succession in Pomerania (northern Poland), *Geol. Quart.,* **44**(3), 297–315.

Jelínek, V. & Pokorný, J. 1997. Some new concepts in technology of transformer bridges for measuring susceptibility anisotropy of rocks, *Phys. Chem. Earth,* **22**(1-2), 179–181.

Jeppsson, L. & Calner, M. 2002. The Silurian Mulde Event and a scenario for secundo–secundo events, *Earth Environ. Sci. Trans. R. Soc. Edinburgh,* **93**(02), 135–154.

Johnson, M.E. 1996. Stable cratonic sequences and a standard for Silurian eustasy, in *Paleozoic sequence stratigraphy; views from the North American Craton,* Vol. **306,** eds Witzke, B. J., Ludvigson, G. A. & Day, J., Geological Society of America Special Papers.

Johnson, M.E. 2006. Relationship of Silurian sea-level fluctuations to oceanic episodes and events, *GFF -Uppsala,* **128,** 115–121.

JohnsoN, M.E. 2010. Tracking Silurian eustasy: alignment of empirical evidence or pursuit of deductive reasoning?, *Palaeogeogr. Palaeoclimatol. Palaeoecol.,* **296,** 276–284.

Johnson, M.E., Rong, J. & Kershaw, S. 1998. Calibrating Silurian eustasy against the erosion and burial of coastal paleo topography, *N. Y. State Museum Bull.,* **491,** 3–13.

Kąkol, Z. & Honig, J.M. 1989. Influence of deviations from ideal stoichiometry on the anisotropy parameters of magnetite $Fe_3(1\text{-}\delta)O_4$, *Phys. Rev. B,* **40,** 9090–9097.

Kąkol, Z., Sabol, J., Stickler, J., Kozłowski, A. & Honig, J.M. 1992. Influence of titanium doping on the magnetocrystalline anisotropy of magnetite, *Phys. Rev. B,* **49,** 12 767–12 772.

Karlin, R. 1990. Magnetic Mineral Diagenesis in Suboxic Sediments at Bettis Site W-N, NE Pacific Ocean, *J. geophys. Res.,* **95**(B4), 4421–4436.

Karlin, R. & Levi , S. 1983. Diagenesis of magnetic minerals in recent hemipelagic sediments, *Nature,* **303,** 327–330.

Kars, M., Aubourg, C., Labaume, P., Bierquó, T. & Cavailhes, T. 2014. Burial diagenesis of magnetic minerals: New insights from the Grès d'Annot Transect (SE France), *Minerals,* **4**(3), 667–689.

MKars, ., Aubourg, c. & Suárez-Ruiz, I. 2015. Neoformed magnetic minerals as an indicator of moderate burial: The key example of middle Paleozoic sedimentary rocks, West Virginia, *AAPG Bull.,* **99**(03), 389–401.

Kiipli, E., Kallaste, T. & Kiipli, T. 2000. Hematite and goethite in Telychian marine red beds of the East Baltica, *GFF,* **122,** 281–286.

Kletetschka, G. & Wasilewski, P.J. 2002. Grain size limit for SD hematite, *Phys. Earth planet. Inter.,* **129,** 173–179.

Konon, A. 2004. Successive episodes of normal faulting and fracturing resulting from progressive extension during the uplift of the Holy Cross Mountains, Poland, *J. Struct. Geol.,* **26**(3), 419–433.

Konon, A. 2007. Strike-slip faulting in the Kielce Unit, Holy Cross Mountains, central Poland, *Acta Geol. Polonica,* **57**(4), 415–441.

Konon, A. & Mastella, L. 2001. Structural evolution of the Gnieździska syncline - regional implications for the Mesozoic margin of the Holy Cross Mountains (central Poland), *Ann. Soc. Geol. Poloniae,* **71,** 189–199.

Kopp, R.E. & Kirschvink, J.L. 2008. The identification and biogeochemical interpretation of fossil magnetotactic bacteria, *Earth-Sci. Rev.,* **86**(1–4), 42–61.

Kowalczewski, Z. 1971. Podstawowe problemy geologiczne dewonu dolnego Gór Świętokrzyskich, *Kwartalnik Geologiczny,* **15**(2), 263–283.

Kozłowski, W, Domańska, J., Nawrocki, J. & Pecskay, Z. 2004. The provenance of the Upper Silurian greywackes from the Holy Cross Mountains (Central Poland), in *Proceedings of the 11th Meeting of the Petrology Group of the Mineralogical Society of Poland,* Vol. **24,** pp. 251–254,Karwowski Ł. & Ciesielczuk, J., *Mineralogical Society of Poland – Special Papers*.

Kozłowski, W. 2003. Age, sedimentary environment, and palaeogeographical position of the Late Silurian oolitic beds in the Holy Cross Mountains (Central Poland), *Acta Geol. Polonica,* **53**(4), 341–357.

Kozłowski, W. 2008. Lithostratigraphy and regional significance of the Nowa Słupia Group (Upper Silurian) of the Łysogóry Region (Holy Cross Mountains, Central Poland), *Acta Geol. Polonica,* **58**(1), 43–74.

Kozłowski, W., DomańSka-Siuda, J. & Nawrocki, J. 2014. Geochemistry and petrology of the Upper Silurian greywackes from the Holy Cross-Mountains (central Poland): Implications for the Caledonian history of the southern part of the Trans-European Suture Zone (TESZ), *Geol. Quart.,* **58,** 311–336.

Kremer, B. 2005. Mazuelloids: product of post-mortem phosphatization of enantiomorphic acritarchs, *Palaios,* **20,** 27–36.

Kruiver, P. P., Dekkers, M. J. & Langereis, C. G. 2000,Secular variation in Permian red beds from Dôme de Barrot SE France, *Earth planet. Sci. Lett.,* **179,** 205–217.

Krzywiec, P. 2002. Mid-Polish Trough inversion - seismic examples, main mechanisms, and its relationship to the Alpine – Carpathian collision. W: Bertotti, G. (red.), Continental Collision and the Tectonosedimentary Evolution of Forelands: Mechanics of Coupling and Far-field Deformation, *Eur. Geophys. Soc. Spec. Publ.,* **1,** 151–165.

Krzywiec, P. 2007. Tectonics of the Lublin area (SE Poland) - new views based on results of seismic data interpretation, *Biuletyn Państwowego Instytutu Geologicznego,* **422** (in Polish with English summary), 1–18.

Krzywiec, P., Gutowski, J., Walaszczyk, I., Wróbel, G. & Wybraniec, S. 2009. Tectonostratigraphic model of the Late Creetaceous inversion along the Nowe Miasto-Zawichost Fault Zone SE Mid-Polish Trough, *Geol. Quart.,* **53,** 27–48.

Kutek, J. & Głazek, J. 1972. The Holy Cross area, Central Poland, in the Alpine cycle, *Acta Geol. Polonica,* **22,** 603–653.

LamarchE, J. *et al.* 1999. Variscan tectonics in the Holycross Mountains (Poland) and the role of structural inheritance during Alpine tec-tonics, *Tectonophysics,* **313**(1–2), 171–186.

Lamarche, J., BergeraT, F., Lewandowski, M., Mansy, J.L., Świdrowska, J. & Wieczorek, J. 2002. Variscan to Alpine heterogeneous palaeo-stress field above a major Palaeozoic suture in the Carpathian foreland (southeastern Poland), *Tectonophysics,* **357**(1–4), 55–80.

Lamarche, J., Lewandowski, M., Mansy, J. L. & Szulczewski, M. 2003a. Partitioning pre-, syn-and post-Variscan deformation in the Holy Cross Mountains, eastern Variscan foreland, *Geol. Soc., Lond., Spec. Publ.,* **208,** 159–184.

Lamarche, J., Scheck, M. & Lewerenz, B. 2003b. Heterogeneous tectonic inversion of the Mid-Polish Trough is related to crustal architecture, sedimentary patterns, and structural inheritance, *Tectonophysics,* **373,** 75–92.

Lewandowski, M. 1993. Paleomagnetism of the Paleozoic rocks of the Holy Cross Mts (Centrol Poland) and the origin of the Variscan orogen, *Publ. Inst. Geophys. Pol. Acad., A,* **23**(265), 1–85.

Lewandowski , M. 1994. Palaeomagnetic constraints for Variscan mobilism of the Upper Silesian and Malopolska Massifs, southern Poland, *Geol. Quart.,* **38**(2), 211–230.

Liu, J., Zhu , R., Roberts, A.P., Li, S. & Chang, J.-H. 2004. High-resolution analysis of early diagenetic effects on magnetic minerals in post-middle-Holocene continental shelf sediments from the Korea Strait, *J. geophys. Res.,* **109**(B3), doi:10.1029/2003JB002813.

Liu, Q., Yu, Y., Torrent, J., Roberts, A. P., Pan, Y. & Zhu, R. 2006. Characteristic low-temperature magnetic properties of aluminous goethite [a-(Fe, Al)OOH] explained, *J. geophys. Res.,* **111**(B12), doi:10.1029/2006JB004560.

Lowrie, W. 1990. Identification of ferromagnetic minerals in a rock by coercivity and unblocking temperature properties, *Geophys. Res. Lett.,* **17**(2), 159–162.

Malec, J. 1993. Upper Silurian and Lower Devonian in the western Holy Cross Mts, *Geol. Quart.,* **37**(4), 501–536.

Malec, J. 2000. Wyniki badań sedymentologicznych szarogłazów górnego syluru w rejonie Niestachowa, *Pos. Nauk. Państw. Inst. Geol.,***56,** 92–95.

Malec, J., Kuleta, M. & Migaszewski, Z. 2016. Lithologic-petrographic characterization of Silurian rocks in the Niestachów profile (Holy Cross Mountains), *Annales Societatis Geologorum Poloniae,* **86,** 85–110.

Malinowski, M., Żelaźniewicz, A. Grad, M. Guterch, A. & Janik, T. 2005. Seismic and geological structure of the crust in the transition from Baltica to Palaeozoic Europe in SE Poland—CELEBRATION 2000 experiment, profile CEL02, *Tectonophysics,* **401**(1–2), 55–77.

Marynowski, L. 1999. Thermal maturity of organic matter in Devonian rocks of the Holy Cross Mts. (Central Poland), *Przegląd Geologiczny,***47,** 1125–1129.

Marynowski, L., Czechowski, F. & Simoneit, B. R. T. 2001. Phenylnaphthalenes and polyphenols in Palaeozoic source rocks of the Holy Cross Mountains, Poland, *Organ. Geochem.,* **32,** 69–85.

Marynowski, L., Pisarzowska, A., Derkowski, A., Rakociński, M., Szaniawski, R., Środoń, J. & Cohen, A. S. 2017. Influence of palaeoweathering on trace metal concentrations and environmental proxies in black shales, *Palaeogeogr., Palaeoclimatol., Palaeoecol.,* **472,** 177–191.

Marynowski, L., Salamon, M. & Narkiewicz, M. 2002. Thermal maturity and depositional environments of organic matter in the post-Variscan succession of the Holy Cross Mountains, *Geol. Quart.,***46,**25–36.

Masiak, M., Podhalańska, T. & Stempień-Sałek, M. 2003. The Ordovician-Silurian boundary in the Bardo Syncline, Holy Cross Mountains, Poland - new data on fossil assemblages and sedimentary succession, *Geol. Quart.,* **47**(4), 311–330.

Mastella, L. & Konon, A. 2002. Non-planar strike-slip Gnieździska – Brzeziny fault (SW Mesozoic margin of the Holy Cross Mountains, central Poland), *Acta Geol. Polonica,* **52**(4), 471–480.

Maxbauer, D.P., Feinberg, J.M. & Fox, D.L. 2016. MAX UnMix: a web application for unmixing magnetic coercivity distributions, *Comput. Geosci.,* **95,** 140–145.

Mazur, S., Scheck-Wenderoth, M. & Krzywiec, P. 2005. Different modes of the Late Cretaceous-Early Tertiary inversion in the North German and Polish basins, *Int. J. Earth Sci.,* **94,** 782–798.

Mizerski, W. 1979. Tectonic of the Łysogóry Unit in the Holy Cross Mts, *Acta Geol. Polonica,* **29,** 1–38.

Mizerski, W. 1995. Geotectonic evolution of the Holy Cross Mts in central, *Europe. Biuletyn Państw. Inst. Geol.,* **327,** 1–47.

Mizerski, W. 2004. The Holy Cross Mountains in the Caledonian, Variscan, and Alpine cycles — major problems, open questions, *Przegląd Geologiczny,* **52**(8/2),774–779.

Moskowitz, B.M., Frankel, R.B. & Bazylinski, D.A. 1993. Rock magnetic criteria for the detection of biogenic magnetite, *Earth planet. Sci. Lett.,* **120,** 283–300.

Moskowitz, B.M., Jackson, M. & Kissel, C. 1998. Low-temperature magnetic behavior of titanomagnetites, *Earth planet. Sci. Lett.,* **157**(3–4), 141–149.

Mustafa, K. A., Sephton, M. A, Watson, J. S., Spathopoulos, F. & Krzywiec, P. 2015. Organic geochemical characteristics of black shales across the Ordovician–Silurian boundary in the Holy Cross Mountains, central Poland, *Mar. Petrol. Geol.,* **66**(4), 1042–1055.

Naglik, B., Toboła, T., Natkaniec-Nowak, L., Luptakova, J. & Milovska, S. 2016. Raman spectroscopic and microthermometric studies of authigenic quartz (the Pepper Mts., Central Poland) as an indicator of flu-ids circulation, *Spectrochim. Acta Part A: Mol. Biomol. Spectrosc.,* **173,** 960–964.

Narkiewicz, M. 2002. Ordovician through earliest Devonian development of the Holy Cross Mts. (Poland): constraints from subsidence analysis and thermal maturity data, *Geol. Quart.,* 2002, **46**(3), 255–266.

Narkiewicz, M. 2017. Comment on a paper by Schito et al. (2017) "Thermal evolution of Paleozoic successions of the Holy Cross Mountains (Poland)", *Mar. Petrol. Geol.,* **88,**1109–1113.

Narkiewicz, M., Racki, G., Skompski, S. & Szulczewski , M. 2006. Records of processes and events in the Devonian and Carboniferous of the Holy Cross Mountains, in *Proceedings of the 77th Meeting of the Polish Geological Society, Conference Volume,* pp. 51–77( in Polish).

Narkiewicz, M., Resak, M., Littke, R. & Marynowski, L. 2010. New constraints on the Middle Palaeozoic to Cenozoic burial and thermal history of the Holy Cross Mts. (central Poland): Results of numerical modeling, *Geol. Acta,* **8,** 189–205.

Nawrocki, J. *et al.* 2007. Late Neoproterozoic to Early Palaeozoic palaeogeography of the Holy Cross Mountains (Central Europe): an integrated approach, *J. Geol. Soc.,* **164,** 405–423.

Nawrocki, J. & Poprawa, P. 2006. Development of Trans-European Suture Zone in Poland: from Ediacaran rifting to Early Palaeozoic accretion, *Geol. Quart.,* **50,** 59–76.

Niezabitowska, D. K., Szaniawski, R., Roszkowska-Remin, J. & Gąsiński, A. 2019a. Magnetic anisotropy in Silurian gas-bearing shale rocks from the Pomerania region (northern Poland), *J. geophys. Res.,* **124,** 5–25.

Niezabitowska, D.K., Szaniawski, R. & Jackson, M. 2019b. Magnetic mineral assemblage as a potential indicator of the depositional environment in gas-bearing Silurian shales from Northern Poland, *Geophys. J. Int.,* **218**(2), 1442–1455.

Oches, E.A. & Banerjee, S.K.. 1996. Rock-magnetic proxies of climate change from loess-paleosol sediments of the Czech Republic, *Stud. Geophys. Geod.,* **40,**287–300.

Özdemir, D. 1990. High-temperature hysteresis and thermoremanence of single-domain maghemite, *Phys. Earth planet. Inter.,* **65,** 125–136.

Özdemir, D. & Banerjee, S.K. 1984. High-temperature stability of maghemite, *Geophys. Res. Lett.,* **11,** 161–164.

Özdemir, D. & Dunlop, D. J. 1988. Crystallization remanent magnetization during the transformation of maghemite to hematite, *J. geophys. Res.,* **93,** 6530–6544.

Özdemir, Ö. & Dunlop, D. 1996. Thermoremanence and Néel temperature of goethite, *Geophys. Res. Lett.,* **23,** 921–924.

Özdemir, Ö., Dunlop, D.J. & Berquo´, T. S. 2008. Morin transition in hematite: size dependence and thermal hysteresis, *Geochem. Geophys. Geosyst.,* **9**(10), doi:10.1029/2008GC002110.

Özdemir, Ö., Moskowitz, B.M. & Dunlop, D.J. 1993. The effect of oxidation on the Verwey transition in magnetite, *Geophys. Res. Lett.,* **20,** 1671–1674.

Page, A.A., Zalasiewicz, J.A., Williams, M., Popov, L.E. & Gregory, F.J. 2007. Were transgressive black shales a negative feedback modulating glacioeustasy in the Early Palaeozoic Icehouse?, in *Deep-Time Perspective on Climate Change: Marrying the Signal from Computer Models and Biological Proxies,* pp. 123–156, eds Williams, M., Haywood, A.M. & Schmidt, D.N. , The Micropalaeontological Society, Special Publications, The Geological Society.

Passier, H.F. & Dekkers, M.J. 2002. Iron oxide formation in the active oxidation front above sapropel S1 in the eastern Mediterranean Sea as derived from low-temperature magnetism, *Geophys. J. Int.,* **150,** 230–240.

Poprawa, P. 2006. Rozwój kaledońskiej strefy kolizji wzdłuż zachodniej krawędzi Baltiki oraz jej relacje do basenu przedpola, *Prace Państwowego Instytutu Geologicznego,* **186,** 189–214.

Poprawa, P., Kosakowski, P. & Wróbel, M. 2010. Burial and thermal history of the Polish part of the Baltic region, *Geol. Quart.,* **54**(2), 131–142.

Poprawa, P., Šliaupa, S., Stephenson, R. & Lazauskienė, J. 1999. Late Vendian–Early Palæozoic tectonic evolution of the Baltic Basin: regional tectonic implications from subsidence analysis, *Tectonophysics,* **314**(1–3), 219–239.

Poprawa, P., Żywiecki, M. & Grotek, I. 2005. *Burial and thermal history of the Holy Cross Mts. area: a preliminary results of maturity modeling,* Polskie Towarzystwo Mineralogiczne-Prace Specjalne, **26,** 251–254.

PożaryskI, W. 1990. Kaledonidy środkowej Europy - orogenem przesuwczym złożonym z terranów, **38**(1), 441.

Pożaryski, W. 1991. The strike-slip terrane model for the North German-Polish Caledonides, *Publ. Inst. Geoph., Pol. Acad., A ,* **19,** 3–15.

Przepiera, K. & Przepiera, A. 2003. Thermal transformations of selected transition metals oxyhydroxides, *J. Therm. Anal. Cal.,* **74,** 659–666.

Radzevičius, S., Raczyński, P., Užomeckas, M., Norkus, A. & Spiridonov, A. 2019. Graptolite turnover and $\delta$13Corg excursion in the upper Wenlock shales (Silurian) of the Holy Cross Mountains (Poland), *Geologica Carpathica,* **70,** 3, 209–221.

Robinson , S.G., Sahota, J.T.S. & Oldfield, F. 2000. Early diagenesis in North Atlantic abyssal plain sediments characterized by rock-magnetic and geochemical indices, *Mar. Geol.,* **163**(1–4), 77–107.

Ruan, H. D., Frost, R. L. & Kloprogge, J. T. 2001. The behavior of hydroxyl units of synthetic goethite and its dehydroxylated product hematite, *Spectrochim. Acta, A,* **57,** 2575–2586.

Scheck-Wenderoth, M., Krzywiec, P., Zülke, R., Maystrenko, Y. & Frizheim, N. 2008. Permian to Cretaceous tectonics, in *The Geology of Central Europe,* pp. 999–1030, ed. McCann, T., Geological Society of London.

Schito, A., Corrado, S., Trolese, M., Aldega, L., Caricchi, C., Cirilli, S. & Valentim, B. 2017. Assessment of thermal evolution of Palaeozoic successions of the Holy Cross Mountains (Poland), *Mar. Petrol. Geol.,* **80,** 112–132.

Schwartz, M., Lund, S. P., Hammond, D. E., Schwartz, R. & Wong, K. 1997. Early sediment diagenesis on the Blake/Bahama Outer Ridge, North Atlantic Ocean, and its effects on sediment magnetism, *J. geophys. Res.,* **102,** 7903–7914.

Schwarz, E.J. 1975. *Magnetic Properties of Pyrrhotite and their Use in Applied Geology and Geophysics,* Geological Survey Canada.

Schwertmann, U. & Murad, E. 1983. Effect of pH on the formation of goethite and hematite from ferrihydrite:, *Clays Clay Miner.,* **31,** 277–284.

Smolarek, J., Marynowski, L., Spunda, K. & Trela, W. 2014. Vitrinite equivalent reflectance of Silurian black shales from the Holy Cross Mountains, Poland, *Mineralogia,* **45,** 79–96.

Smolarek, J., Trela, W., Bond, D.P.G. & Marynowski, L. 2017. Lower Wenlock black shales in the northern Holy Cross Mountains, Poland: sedimentary and geochemical controls on the Ireviken Event in a deep marine setting, *Geol. Mag.,* **154**(2), 247–264.

Środoń, J. & Trela, W. 2012. Preliminary clay mineral data on burial history of the Holy Cross Mts. Poland, *Mineralogia – Special Papers,* **39,** 93–94.

Stupnicka, E. 1988. Polish Caledonides and their relation to the other European Caledonides. A discussion, *Annales Societatis Geologorum Poloniae,* **58,** 481–485.

Świdrowska, J. & Hakenberg, M. 2008. Evolution of the Mesozoic basins on the southwestern edge of the East European Craton (Poland, Ukraine, Moldova, Romania), *Studia Geologica Polonica,* **130,** 3–130.

Syono, Y. 1965. Magnetocrystalline anisotropy and magnetostriction of $Fe_3O_4$-$Fe_2TiO_4$ series, with special application to rock magnetism, *Jpn. J. Geophys.,* **4,** 71–143.

Szaniawski, R. 2008. Late Paleozoic geodynamics of the Małopolska Massif in the light of new paleomagnetic data for the southern Holy Cross Mountains, *Acta Geologica Polonica,* **58**(1), 1–12. Warszawa

Szaniawski, R., Konon, A., Grabowski, J. & Schnabl, P. 2011. Palaeomagnetic age constraints on folding and faulting events in Devonian carbonates of the Kielce Fold Zone (southern Holy Cross Mountains, Central Poland), *Geol. Quart.,* **55**(5), 223–234.

Szczepanik, Z., 1997. Preliminary results of thermal alternation investigations of the Cambrian acritarchs in the Holy Cross Mts, *Geol. Quart.,* **41**(3), 257–264.

Szczepanik, Z., 2007. *Regionalny gradient paleotermiczny w zapisie palinologicznym starszego paleozoiku i dewonu Gór Świętokrzyskich (in Polish), Granice paleontologii, XX konferencja Naukowa Paleobiologów i Biostratygrafów PTG, Materiały konferencyjne, 10–13 September 2007,* Wydział Geologii UW, Warszawa, pp. 129–132.

Szulczewski, M. 1995. Depositional evolution of the Holy Cross Mts. (Poland) in the Devonian and Carboniferous – a review, *Geol. Quart.,* **39**(4), 471–488.

Szulczewski, M., Belka, Z. & Skompski, S. 1996. The drowning of a carbonate platform: an example from the Devonian-Carboniferous of the southwestern Holy Cross Mountains, Poland, *Sediment. Geol.,* **106**(1–2), 21–49.

Tarnowska, M. 1981. Dewon dolny w centralnej części Gór Świętokrzyskich, *Przewodnik Zjazdu polskiego towarzystwa geologicznego,* **53,** 57–68.

Teller, L. 1997. The subsurface Silurian in the East European platform, *Palaeontol. Pol.,* **56,** 7–21.

Till, J., Guyodo, Y., Lagroix, F., Morin, G. & Ona-Nguema, G. 2015. Goethite as a potential source of magnetic nanoparticles in sediments, *Geology,* **43**(1), 75–78.

Tomczyk, H. 1962. Rastrites forms in the Lower Silurian of the Święty Krzyż Mts, *Bull. Geol. Inst.,* **174**(5), 65–92.

Tomczyk, H. 1970. Silurian, in *Stratigraphy, Precambrian and Palaeozoic,* Vol. 1, Geology of Poland, pp. 237–319, eds Sokołowski, S., Cieślinski, S. & Czerwiński, J., Wydawnictwa Geologiczne.

TomczyK, H., Pajchlowa, M. & Tomczykowa, E. 1977. Poland, in *The Silurian-Devonian Boundary,* lUGS, Ser. A no. 5, pp. 65–83.

Tomczykowa, E. 1958. Fauna z łupków graptolitowych syluru niecki bardziańskiej Gór Świętokrzyskich, *Geol. Quart.,* **2**(2), 321–346.

Tomczykowa, E. & Tomczyk, H. 1981. Rozwój badań syluru w Górach Świętokrzyskich, in *LIII Meeting of the Polish Geological Society, PTG, Kielce 1981,* pp. 42–56, ed. Żakowa, H., Wydawnictwa Geologiczne.

Tomczykowa, E. & Tomczyk, H. 2000. The Lower Palaeozoic in the Daromin IG-1 borehole – Confirmation of the concept of the terrane structure of the Łysogóry and Małopolska blocks (Góry Świętokrzyskie Mts), *Biuletyn Państwowego Instytutu Geologicznego,* **393,** 167–203.

Torsvik , T. H., Trench, A., Svensson, I. & Walderhaug, H. J.(1993). Palaeogeographic significance of mid-Silurian palaeomagnetic results from southern Britain-major revision of the apparent polar wander path for eastern Avalonia, *Geophys. J. Int.,* **113,** 651–668.

Torsvik, T.H. & Rehnström, E.F. 2003. The Tornquist Sea and Baltica–Avalonia docking, *Tectonophysics,* **362**(1–4), 67–82.

Torsvik, T.H., Robin, L. & Cocks, M. 2017. *Earth History and Palaeogeography,* Cambridge Univ. Press.

Torsvik, T.H., Smethurst, M.A., Meert, J.G., Van der Voo , R., Mckerrow, W.S., Brasier, M.D., Sturt, B.A. & Walderhaug, H.J. 1996. Continental break-up and collision in the Neoproterozoic and Palaeozoic—a tale of Baltica and Laurentia, *Earth-Sci. Rev.,* **40,** 229–258.

Trela, W. 2021. Eustatic and local tectonic impact on the Late Ordovician – early Silurian facies evolution on the SW margin of peri-Baltica (the southern Holy Cross Mountains, Poland), *Geol. Mag.,* **158**(8), 1472–1486.

Trela, W., Podhalańska, T. & Malec, J. 2006. Granica ordowik/sylur w Zbrzy — południowa część regionu kieleckiego Gór Świętokrzyskich, in *Przewodnik 77. Zjazdu Naukowego Pol. Tow. Geol. Procesy i zdarzenia w historii geologicznej Gór Świętokrzyskich,* eds Skompski, S. & Żylińska, A., Państw. Inst. Geol.

Trela, W., Podhalańska, T. & Malec, J. 2015. Wyniki badań litologicznych, stratygraficznych i paleontologicznych. Sylur – litologia i stratygrafia, in *Profile Głębokich Otworów Wiertniczych – Wilków 1, Daromin IG 1,* ed. Trela, W., 147pp.

Trela, W., Podhalańska, T., Smolarek, J. & Marynowski, L. 2016. Llandovery green/grey and black mudrock facies of the northern Holy Cross Mountains (Poland) and their relation to early Silurian sea-level changes and benthic oxygen level, *Sediment. Geol.,* **342,** 66–77.

Trela, W. & Salwa, S. 2007. Litostratygrafia dolnego syluru w odsłonięciu Bardo Stawy (południowa część Gór Świętokrzyskich): związek ze zmianami poziomu morza i cyrkulacją oceaniczną, *Przegląd Geologiczny,* **55,** 971–978.

Van der Zee, C., Roberts, D.R., Rancourt , D.G. & Slomp, C.P. 2003. Nanogoethite is the dominant reactive oxyhydroxide phase in lake and marine sediments, *Geology,* **31**(11), 993–996.

Verniers, J., Maletz, J., Kříž, J., Žigait, Ž., Paris, F., Schönlaub, H. P. & Wrona, R. 2008. Silurian, in *The Geology of Central Europe,* Vol. **1,** pp. 249–302, ed. McCann, T., The Geological Society.

Volk, M.W.R., Gilder, S.A. & Feinberg, J.M. 2016. Low-temperature magnetic properties of monoclinic pyrrhotite with particular relevance to the Besnus transition, *Geophys. J. Int.,* **207,** 1783–1795.

Wenk, H.-R., Kanitpanyacharoen, W. & Voltolini , M. 2010. The preferred orientation of phyllosilicates: Comparison of fault gouge, shale, and schist, *J. Struct. Geol.,* **32**(4), 478–489.

Winchester, J.A., Pharaoh, T.C. & Verniers, J. 2002. Palaeozoic amalgamation of Central Europe: an introduction and synthesis of new results from recent geological and geophysical investigations, *Geol.l Soc. Lond., Spec. Publ.,* **201,** 1–18.

Witzke, B.J. 1992. *Silurian Stratigraphy and Carbonate Mound Facies of Eastern Iowa: Field Trip Guidebook to Silurian Exposures in Jones and Linn Counties,* Guidebook Series, Iowa Department of Natural Resources, Energy and Geological Resources Division, Geological Survey Bureau, 111pp.

Yamazaki, T., Abdeldayem, A.L. & Ikehara, K. 2003. Rock-magnetic changes with reduction diagenesis in Japan Sea sediments and preservation of geomagnetic secular variation in inclination during the last 30, 000 years, *Earth Planets Space,* **55,** 327–340.

Znosko, J. 1986. Polish Caledonides and their relation to other Caledonides, *Ann. Soc. Geol. Pol.,* **56,** 33–52.

Znosko, J., 2000. New, unknown data on Caledonian-alpinotype folding in the Holy Cross Mts.(central Poland), *Przegląd Geologiczny,* **48**(5), 401–408.